

THE PROPAGATION OF MEDIUM PRESSURE
DISTURBANCES IN HIGH SUBSONIC
AIR FLOW

J. D. JEFFREY

1951

U. S. Naval Postgraduate School
Monterey, California



THE PROPAGATION OF MEDIUM PRESSURE
DISTURBANCES IN HIGH SUBSONIC AIR FLOW

by

J. D. Jeffrey

Submitted to the Faculty of Sennseler
Polytechnic Institute in partial fulfillment
of the requirements for the degree,
Master of Mechanical Engineering

May 28, 1951

11/10/19
T4

INDEX

	Page
Summary	
Nomenclature	
Introduction	1
Equipment and Procedure	3
Results and Discussion	11
Conclusions and Recommendations	20
References	22
Appendix I:	
Flow Tube Design Considerations	AI-1
Appendix II:	
Flush-Mounted Pressure Pickup Design and Analysis	AII-1
Appendix III:	
Derivation of the Pressure Wave Velocity Equation	AIII-1
Tables	
Figures	



SUMMARY

This study was organized to investigate the physical and theoretical aspects of pressure wave propagation in high velocity subsonic air.

The laboratory phase of the investigation required the design of a flow tube to give a constant Mach number and highly responsive pressure pickups for use with electronic amplification and recording. Pressure disturbances of controlled magnitude were introduced into the flow tube by rupture of a plastic diaphragm used to seal a compression chamber.

For various shock pressures released into the tube, accurate measurements were made as to the time required for the waves to traverse the test length of tube upstream, and the magnitudes of the pressures involved. Within the wave front there was found to exist a pressure peak exceeding in magnitude the normal pressure P_2 following such a disturbance.

In theory, starting with the basic equations of continuity, momentum, and energy, an equation was developed for the absolute velocity of the disturbance front. Essentially the normal plane shock pressure ratio-velocity equation was found to describe the phenomenon with corrections for tube flow velocity and the two existent energy systems - those of the tube flow and of the compression chamber.

One method of analyzing the magnitude of the pressure peak within the shock wave was considered. It was seen from tests that the pressure peak underwent a form of diffusion in moving upstream



into a smaller tube area at a supersonic rate relative to the tube flow.

This project was carried out during the year 1950-51 by the author at Rensselaer Polytechnic Institute, Troy, New York. The laboratory tests were conducted in the high velocity air laboratory of the Mechanical Engineering Department of the school.

NOMENCLATURE

A	Flow area of tube.
P ₁	Pressure ahead of disturbance, normally tube flow static pressure.
P ₂	Pressure behind disturbance.
P _e	Explosion chamber pressure.
P _t	Peak pressure occurring within disturbance.
v	Velocity in ft/sec. of normal tube flow.
w	Velocity in ft/sec. of disturbance front relative to normal tube flow.
u	Absolute velocity of disturbance front.
M	Mach number of normal tube flow.
N	Introduced here as $w / \sqrt{g \gamma R T_0}$
T ₀	Total temperature with regard to normal tube flow, M.
P ₀	Total pressure with regard to normal tube flow.
T _{0'}	Total temperature associated with relative flow, N.
P _{0'}	Total pressure associated with relative flow.
γ	Ratio of specific heats, $c_p/c_v = 1.4$.
Δt	Time in seconds for disturbance front to traverse tube.
f	Friction factor associated with hydraulic radius.
m	Hydraulic radius. Flow area divided by wetted perimeter.
	Wall angle of tube.
Upstream	Refers to the measuring station two inches from throat.
Downstream	Refers to measuring station 26 inches from throat.

Nomenclature of Appendix II is defined and used in that section only.

THE PROPAGATION OF MEDIUM PRESSURE DISTURBANCES IN HIGH SUBSONIC AIR FLOW

INTRODUCTION

In the past, considerable experimentation and theorizing has been done on the shock tube which sends a compression wave into still air and a rarefaction into the compression chamber. Altho this problem is still being investigated, its characteristics are fairly well established.

The next logical step, which was undertaken by the work as described in this report, was to introduce medium pressure disturbances into moving air and to observe their characteristics as the waves moved upstream. Practically, such an investigation would serve to add to the knowledge of sudden energy changes as are evident in shock fronts, and would find related application in situations as quick-closing and opening control valves used on air drive for light auxiliary turbine wheels.

In scope, this investigation was considered to be a primary overall physical survey of the problem. Pressure disturbances of varying intensity were introduced into air flow in a tube of average Mach number 0.8.

Desired data included velocity of the moving wave front, pressure ratio across the front, and peak pressure in the front for

each intensity of applied disturbance. To obtain this data, a special dynamic pressure pickup was designed as one phase of the laboratory part of this investigation.

The theory of the observed phenomenon was developed from the basic flow equations of continuity, momentum, and energy relative to the shock front. Superposition was employed to account for the added effect of tube flow. This approach was indicated as the most feasible way to get "engineering" answers since a mathematical treatment accounting for all variables simultaneously would be very complex and might well in itself be the scope of a complete investigation.

This investigation was conducted by the author during the course of the school year 1950-51 in the high velocity air laboratory of the Mechanical Engineering Department at Rensselaer Polytechnic Institute, Troy, New York.

The author is indebted to many individuals for their contributions to the design and use of the laboratory equipment. Specific acknowledgement is given with thanks to Prof. W. P. Bailey for many suggestions on the overall laboratory set-up; to Prof. R. H. Trathen on the application of strain gages; and to Mr. Waldo Goyer of the Mechanical Engineering Department metal working shop for his fine craftsmanship.



EQUIPMENT AND PROCEDURE

Fig. 1 is a schematic drawing of the complete laboratory test arrangement and Fig. 6 a photograph of the test setup.

The laboratory equipment divided itself naturally into four basic groups; compressors and other laboratory fixtures, the flow tube, shock producing mechanism, and dynamic pressure pickups with the required electronic equipment. Each group will be described in detail with emphasis on the specially designed items.

Group A: Compressors and basic laboratory equipment.

Air was supplied by two six-cylinder Shram compressors, model 210, rated at 206 cubic feet of standard air per minute at 1175 RPM. A Westinghouse three phase, 60 cycle, 220 volt, 50 horsepower motor with rated full load speed of 1175 RPM was connected by direct drive to each compressor. Air from the compressors went thru aftercoolers into storage tanks with maximum pressure preset for 100 psig.

The combined air from the two storage tanks was piped into a plenum chamber thru coarse and fine control valves in parallel. Located in the plenum chamber was a one inch metering nozzle across which a mercury manometer read pressure drop. In the main compartment of the plenum chamber was a Weston gas thermometer, 0-220° F., and a total pressure tap with line leading to an Ashcroft 0-100 psi pressure gage.

With the known area of the metering nozzle and pressure drop across it, plus total temperature and pressure, the weight flow of air could be determined. No corrections were made to any of the

recorded data from the plenum chamber-metering nozzle combination instruments due to their permanent mounting which made calibration inadvisable, and also due to the fact that all runs were to be made under the same flow conditions.

Group B: Flow tube.

Fig. 2 shows the mounting end of the flow tube and Fig. 7 the tube in position bolted to the face plate of the plenum chamber.

Design considerations are covered in detail in Appendix I. The tube was designed to give an average flow of Mach number 0.8 with weight flow 0.49 lbs/sec.

The tube was 32 inches long from throat to exit, of rectangular cross section with inside dimensions uniformly varying from .7x.9 inches at the throat to 1.1x.9 inches at the exit. The tube proper was fabricated from $\frac{1}{4}$ inch flat brass with sides held together by $\frac{3}{32}$ inch metal screws placed $1\frac{1}{2}$ inches apart. A brass flange on the tube at the throat was bolted to the one inch nozzle section turned from aluminum stock. The nozzle piece had a five inch diameter with eight $\frac{1}{4}$ inch bolt holes drilled in a four inch circle to permit securing to the plenum chamber.

The test section of the tube was that portion between the two inch and the 26 inch station. Static pressure taps were located at 2, 10, 18, and 26 inch stations on one vertical wall to permit tube calibration. Leads from the four taps went to a common manifold to which was attached a mercury manometer. On the opposite tube wall at the two and 26 inch stations were $\frac{3}{4}$ inch taps to permit insertion of either the dynamic pressure pickup or the similar pressure sensing

element. At the $29\frac{1}{2}$ inch station on the bottom tapering wall was the one inch hole for explosion chamber connection with a $1/8$ inch tap directly above for the puncture rod guide.

A detachable exit receiver chamber in the form of a cylinder four inches in diameter and $6\frac{3}{4}$ inches long was clamped over the end of the tube to control the flow characteristics of the tube. Eight $\frac{1}{2}$ inch holes comprised its exit area over which was centered a brass plate with eight similar holes. The outer plate could rotate and thus control the amount of opening and back pressure.

Group C: Shock-producing mechanism.

A considerable problem arose in the question of how to introduce a disturbance into steady flow without interrupting the flow by gadgetry prior to setting it off. Such schemes as detonation of an explosive in an expanded part of the flow tube, or firing a blank cartridge into the end of the tube were considered and rejected due to lack of control or lack of information as to what the effective intensity of the disturbance might be.

Since the application of plastic diaphragms had proven so effectively simple in the case of the straight shock tube, it was decided to adapt them to this case. Fig. 3 shows the exit end of the flow tube with the shock producing mechanism.

The shock pressure chamber was a cylindrical tank with inside dimensions four inches in diameter and 12 inches long. Filling was accomplished by an air hose with chuck flowing thru a conventional automobile tire valve fitted to the tank. The tank had a $\frac{3}{4}$ inch tap normally plugged, into which the dynamic pressure pickup was inserted

for calibration. A U. S. Gage Co. 0-100 psi gage indicated tank pressure. This gage was calibrated by dead weight tester with results shown in Fig. 10.

A flanged one inch pipe with $\frac{1}{2}$ inch inside diameter was screwed into the tank top. The flanged top had cut in it a $1\frac{1}{2}$ inch diameter recess for holding the plastic diaphragm. A mating flanged pipe led to the flow tube. Upon insertion of the diaphragm, the flanged pipe ends were secured together with six $1/8$ inch bolts set in a $2\frac{1}{16}$ inch circle. This arrangement gave a very tight fit with appreciable leakage around the diaphragm only at the higher pressures.

Set in the top surface of the tube was a gland guide thru which a $1/16$ inch puncture rod with sharpened end centered over the diaphragm. A sharp rap on the puncture rod very cleanly ruptured the diaphragm sending the high pressure disturbance in at right angles to the flow in the tube.

Clear cellophane diaphragms of .001, .003, and .005 inches were tried. The .001 inch were effective for tank pressures of 15 to 35 lbs. gage under non-flow conditions but would not stand up under tube flow vibrations long enough for standard test conditions to be established and data taken. The .003 inch plastic was used from 35 to 65 psig tank pressures, and the .005 from 65 to maximum available, about 93 psig.

The tank was filled usually about 10 psi higher than the test pressure desired to allow for leakage while tube flow was being established. It was necessary to fill the tank prior to starting tube flow since only about 50 psig was available for the tank if the



tube were flowing.

Group D: Pressure pickups and electronic recording apparatus.

The dynamic pressure pickup was designed from considerations as given in Appendix II to meet size limitations of the tube and electronic response characteristics of the Hathaway amplifier and oscillograph combination. The pickup, as shown in Fig. 2, is of the flush-mounted type to give the most accurate response with least disturbance to the flow. A .020 inch brass diaphragm was tinned to the base plug leaving a 9/16 inch inner diameter on which to mount the sensitive element. The plug was threaded for $\frac{1}{4}$ inch with a hexagonal top. With the proper washer, the diaphragm was flush with the inner tube wall.

Calculated natural frequency of the pickup was 16,460 cycles per second.

SR-4 Baldwin Southwark type A-8 strain gages, gage factor 1.76, resistance 120 ohms, were selected on the basis of their good temperature characteristics, frequency response (known up to 50,000 cycles), and rugged reliance. The inner diaphragm surface was roughed with very light sandpaper and cleaned with carbon tetrachloride. The strain elements were mounted in the diaphragm center with duco cement and allowed to dry under pressure for a period of 72 hours. One lead from the strain gage went to an insulated terminal, the other grounded to the plug. Two such units were made.

One unit was designated the dynamic pressure pickup and used exclusively with the Hathaway MRC 15 C carrier amplifier to measure actual pressure. This amplifier had a guaranteed flat response from

0-1500 cycles per second. With a dummy gage it formed two external legs of a bridge to which was fed 4200 cycle voltage from a built-in oscillator. Five volt bridge voltage with $\frac{1}{2}$ attenuation was used.

The other unit was used as a pressure change sensing element and formed one leg of an external bridge with two legs 120 ohms and two 500 ohms. The other 120 ohm leg was actually a potentiometer used to balance the bridge. A $23\frac{1}{2}$ volt battery supplied the bridge thru an off-on switch. This element gave output only for a change of pressure when a generated a.c. signal fed into the MRC15AC a.c. amplifier. It was thus used as a time marker at the station opposite the dynamic pickup. This wide band amplifier was designed for use with strain gages and had a guaranteed flat response 3-5000 cycles per second.

The MRC15C and MRC15AC amplifiers were combined into an MRC16 control unit containing amplifiers, power supply, oscillator, and bridge balancing controls. It was manufactured by the Hathaway Instrument Co., Denver, Colo. The two-channel output of the control unit fed to the five-channel Hathaway recording oscillograph S-14A.

The time pulse from the a.c. amplifier fed to the oscillograph channel one with a type OA-2 one ohm galvanometer of natural frequency 5500 cycles and maximum current 500 milliamps.

The dynamic pressure signal fed to channel three with an OA-2 seven ohm galvanometer of natural frequency 3500 cycles and 100 milliamps maximum current.

Recordings from the oscillograph were made on Kodak 809 Linograph paper driven at 40 inches per second.

The dynamic pressure gage was calibrated using the corrected pressure of the tank gage as reference. Calibration is shown in Fig. 11. A recalibration after being used for record runs showed no change from the original.

Fig. 8 is a photo of the component parts of the tube and shock producing mechanism with the pressure pickups and leads.

Procedure.

Nine runs were made with the dynamic gage at the upstream station and six recording from the downstream station. Each series of runs covered the pressure range from about 35 to 85 psig shock tank pressure.

With all the equipment in position and compressors on, the procedural technique for each run involved the adjustment of three separate systems.

First, the electronic system was put in ready condition by adjusting bridge voltage and attenuation, and balancing input and output circuits of the MC150 unit. Then the $22\frac{1}{2}$ volt 60 Hz AC supply was turned on, sensitivity set, and film shutter of the oscillograph opened. These steps represented the minimum preparation for each run. Prior to each series of runs, the pressure pickups, amplifiers, and oscillograph had to be completely checked for operability.

Second, the shock tank was filled to about 10 psig above the desired pressure.

Third, the flow of air thru the tube was set to the predetermined value by adjusting plenum chamber pressure with the entering

air flow valve simultaneously with pressure at the two inch tube station by use of the variable exit area control.

When flow thru the tube had steadied, the shock tank pressure was set, and the run triggered by turning on the master oscillograph switch and tapping the puncture rod to rupture the diaphragm. Altho each run required extensive and careful preliminary steps, actual full operation lasted only about $1\frac{1}{2}$ seconds during which time five feet of film was exposed.

RESULTS AND DISCUSSION

On the Design of Equipment.

As much a part of the results as the oscillograms was the performance of the equipment, in particular the flow tube and the pressure pickups especially designed for this series of experiments.

Fig. 9 shows the tube calibration with and without the exit chamber receiver. The fact that the tube gave supersonic flow with a free exit indicated a critical nozzle section with probable separation of flow at the throat. Three different nozzle entrance configurations were tried with no measurable difference. A reduction on plenum chamber pressure moved the shock back to between the 10 and 18 inch stations. The next change with reduced plenum chamber pressure gave low subsonic flow thruout.

The simple remedy was to exhaust into an exit chamber by which exit area and back pressure could be controlled. This eliminated the supersonic tendency but showed that the tube was actually a diffuser with too much built-in area increase.

The assumed friction factor of .007 was the determining factor in deciding the area change gradient over the length of the tube necessary to give a constant Mach number. The clue to a probable more correct value lies in Fig. 9 showing flow of nearly constant Mach number about 1.2. From Appendix I,

$$\frac{f \delta M^2}{2} = \tan \alpha$$

From this, a value

$$f = \frac{2 \tan \alpha}{\delta M^2} = .00311$$

is indicated. For smooth circular tubes of constant area, f is usually .005 or a little less. In diffusers it supposedly is greater depending on the actual amount of friction and divergence of tube walls. In this case since only enough area increase to give constant Mach number was desired with no diffuser action, a value of .004 to .005 would probably have given the desired flow.

With allowance made for a friction factor of .007, one possible solution was to introduce additional friction. The interior of the tube was coated with shellac and fine sand blown in. The result of this treatment was to give a constant M of slightly greater than .8 between two and ten inches with increasing diffuser action toward the exit. Several different applications of the shellac-sand combination gave generally the same results. The obvious conclusion was that with small cross-sectional area, roughing the walls produced the desired effect, but in the larger areas toward the exit, the added turbulence and friction near the walls did not affect the already turbulent flow.

For record runs it was decided to keep the nearly straight line M variation. Accordingly the tube was cleaned out and used in its original smooth condition.

The measurement of short time transient conditions always raises the question of whether the results are qualitatively and quantitatively correct. If it were possible to calibrate the measuring instrument under the dynamic conditions, then probably the calibration method could be applied to the problem in the first place and instrumentation worries eliminated. Unfortunately no direct



method of dynamic calibration exists.

In the pressure-time measurements of these tests, the frequency chain seemed satisfactory. For the calculated frequency of 16,460 cycles per second of the dynamic pickup, was associated a 4200 cycle bridge voltage, guaranteed amplifier flat response of 1500 cycles, and galvanometer of 3500 cycles natural frequency. The similar pressure change sensing element fed thru a guaranteed flat 5000 cycle a.c. amplifier to a 4500 cycle galvanometer.

From Fig.4, the duration of the transient condition is shown as about 1/1000 second with an intermediate peak at the upstream tube end, while at the shock end, Fig.5, the pressure change P_1 to P_2 is indicated as occurring in about 1/1500 second.

Oscillograph Data.

The oscillograph records, as shown in Figs. 4 and 5, are representative samples of the series taken at each end. Time was measured from the start of the pressure change at each station which in all cases was a well defined break. Pressures were measured with reference to the static pressure P_1 of the normal tube flow at each measuring station ahead of the disturbance.

From the oscillograms, three significant but interrelated items of data were obtained for the different explosion chamber pressures with tube running under the same conditions of average Mach number .727. The peak pressure of the disturbance, the pressure ratio across the disturbance, and the time for the disturbance front to traverse the two foot test section are summarized for each explosion chamber pressure, P_e , in Tables II and III and given in graphical

form on Fig's. 12, 13, and 14.

In Fig. 12, except for run 3 at $P_e = 52.0$, all the peak pressures, P_t , show consistent results with the slopes of the curves decreasing at the higher P_e . At the upstream station there appears to be an asymptotic limit to the peak pressure of about 36 psig.

The $\Delta t - P_2/P_1$ data for run 3 as shown in Fig. 15 appears to be consistent, however. It is apparent that the effective P_e was 38.2 psig rather than 52 probably caused by a partial rather than complete plastic diaphragm rupture on this run.

The absolute pressure ratio magnitudes, before and after shock, with run 3 corrected as before, show relatively smooth data plotted against P_e in Fig. 13. Beginning with a pressure ratio of 1.7 there is an increasing divergence between upstream and downstream readings with increasing P_e . This difference will be analyzed later.

The $\Delta t - P_e$ plot of Fig. 14 was the only plot where the data of all runs could be put into one curve. The smallest time increment measurable was .000125 seconds altho .00025 seconds was a more probable limit for accuracy. In the region of higher explosion pressures, the points showing greater time of traverse, Δt , were taken with the dynamic gage at the upstream station and the shorter times with the dynamic gage at the downstream station. The smooth curve was faired in giving all points equal weight.

In Fig. 15 time of traverse is plotted against pressure ratio across the disturbance. Here some scattering of test data becomes apparent. To see the most probable relation between these two variables, the following procedure was used. For any one Δt , there

was one corresponding explosion chamber pressure. Therefore P_e became a common parameter. From Fig. 13, for each run with its associated P_e , the pressure ratio was corrected to the faired curve. Similarly, in Fig. 14, the time of traverse was corrected to the faired curve at the same P_e . Table IV gives the data for each run so corrected.

The time of traverse was changed into velocity u by dividing the distance of two feet between measuring stations by the Δt . For comparison with theory, it was desired to use a velocity ratio $u/\sqrt{g \gamma R T_0}$ where T_0 is the total temperature of normal tube flow. Since T_1 varies with Mach number thru the tube and T_0' varies with explosion chamber pressure, T_0 is the only available constant temperature parameter on which to base data from all runs.

The data of Table IV, $u/\sqrt{g \gamma R T_0}$ versus P_2/P_1 , is plotted in Fig. 16. For any one value of $u/\sqrt{g \gamma R T_0}$, the corresponding P_2/P_1 values at each measuring station are read as abscissae.

Theory and Test.

From Appendix III, Equation 31 for velocity ratio is developed.

$$\frac{u}{\sqrt{g \gamma R T_0}} = \left(\frac{P_2}{P_0}\right)^{\frac{\gamma-1}{2\gamma}} \sqrt{\frac{2}{\gamma+1} \frac{1 + \frac{\gamma+1}{\gamma-1} \frac{1}{M^2}}{\frac{P_2}{P_1} + \frac{\gamma+1}{\gamma-1}}} - M_1 \sqrt{\frac{1}{1 + \frac{\gamma-1}{2} M_1^2}}$$

$$= (A) (B) - (C)$$

Factor (B) is the basic relation which would hold if flow of u were moving into a stationary shock region. The term (C) accounts for the shock disturbance moving into an opposing flow M_1 .

The additional factor (A) corrects the velocity u for two

existant energy levels; one represented by T_0 the total temperature of normal tube flow, the other by T_0' associated with the disturbance moving at velocity w_1 with respect to tube flow as motivated by the explosion tank pressure.

This expression would give an average velocity for an average P_2/P_1 existing over the test section. The oscillograph records were limited to giving an average velocity. A plot of Eq. 31 was made by using P_e values and the corresponding average P_2/P_1 between upstream and downstream stations from Fig. 13. This gave a curve of shape similar to the upstream test curve of Fig. 16 which immediately indicated that pressure ratio data from the downstream station near the shock inlet was not truly representative of pressures on either side of a normal shock front.

Eq. 31 was replotted for various P_2/P_1 using the corresponding shock tank pressure which gave each pressure ratio at the upstream station. From Fig. 16 it may be seen that this theoretical treatment is in close agreement with test data. Friction, which is a function of physical flow, and the heat transfer involved in the shock pressure tank were not incorporated into the theoretical equation.

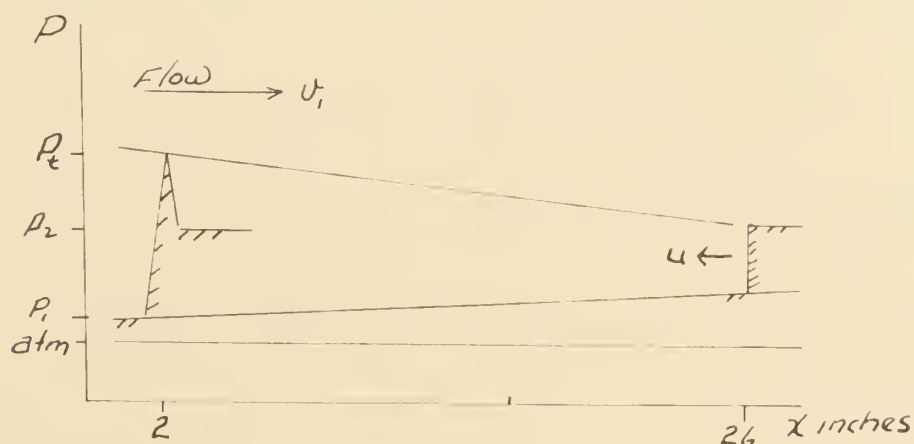
In discussing the shock tube utilizing a plastic diaphragm rupture, Ref. (E) states that the tube gives a plane shock wave, the shock is not greatly attenuated in travelling up the tube, and turbulence effects are small for some distance behind the shock. If these statements be assumed to apply to the current shock investigation problem, the considerable attenuation of the shock strength

P_2/P_1 shown in Fig. 16 is again indicated to be unreasonable.

In reexamining the data taken at the downstream station, typical of which is Fig. 5, the pressure labelled P_2 can now be seen in a dual role. Since, with but slight increase, it persisted until after the disturbance reached the upstream station, it was assumed that it was the P_2 associated with pressure change thru a normal shock front. However, in the light of the foregoing analysis, it is more probable that this P_2 is the peak pressure of the disturbance transmitted down the tube and corresponding to the P_t as observed at the upstream station.

It is concluded that the P_2/P_1 downstream data plotted in Figs. 17, 15, and 16 does not represent the pressure ratio associated with normal shock fronts which is the pressure ratio used to explain the velocity of wave propagation here existant. The downstream measuring station was $3\frac{1}{2}$ inches from the shock inlet. This distance was apparently too close for the pressure wave to develop into the shape as shown in Fig. 4 for the upstream station.

From the data available, the wave shape of the pressure disturbance as it moves up the tube is shown as



For given tube flow conditions, P_2/P_1 has been shown to be the factor governing velocity of the disturbance.

In Ref. (2) and others dealing with the straight shock tube, oscillograph records show no such peak as is brought out in Fig. 4 between P_1 and P_2 . Their wave front is simply pictured as a pressure step from P_1 to P_2 . This is reasonable since only one energy level exists. The element of the opposing kinetic energy is not present as it is in the current situation.

The peak pressure might be viewed as resulting from the acceleration of air at rest in the explosion chamber at pressure P_e to the hypothetical velocity $w_1 = u + v_1$ in air at rest with temperature and pressure corresponding to total temperature and pressure of the actual tube flow.

In terms of conventional air flow, from Ref. (A), such an acceleration would result in the pressures and Mach number expressed by

$$\left(\frac{P_0}{P}\right)^{\frac{\gamma-1}{\gamma}} = \frac{\gamma-1}{2} \left[M^2 + \frac{2}{\gamma-1} \right]$$

Adapting this to the special case at hand

$$\left(\frac{P_0'}{P_t}\right)^{\frac{\gamma-1}{\gamma}} = \frac{\gamma-1}{2} \left[N^2 + \frac{2}{\gamma-1} \right]$$

where N is introduced and defined as

$$N^2 = \frac{w_1^2}{\gamma \gamma R T_0}$$

In Appendix III, Eq. 34, the velocity pressure ratio relation is developed as:

$$\frac{w_1^2}{\gamma \gamma R T_0} = \frac{(\gamma+1) \frac{P_2}{P_1} K^{\gamma-1}}{2 \gamma} \left(\frac{T_1}{T_0} \right)$$

or

$$N' = \frac{(\gamma+1) \frac{P_2}{P_1} + (\gamma-1)}{2\gamma} \left(\frac{T_1}{T_0} \right)$$

With T_1/T_0 that of the normal tube flow.

Then

$$\left(\frac{P_0'}{P_t} \right)^{\frac{\gamma-1}{\gamma}} = \frac{\gamma-1}{2} \left[\frac{(\gamma+1) \frac{P_2}{P_1} + (\gamma-1)}{2\gamma} \left(\frac{T_1}{T_0} \right) \right] + 1$$

and

$$P_t = \frac{P_0'}{\left\{ \frac{\gamma-1}{2} \left[\frac{(\gamma+1) \frac{P_2}{P_1} + (\gamma-1)}{2\gamma} \frac{T_1}{T_0} \right] + 1 \right\}^{\frac{\gamma}{\gamma-1}}}$$

If P_0' is considered to be $(P_0 + P_e)$ in terms of absolute pressure, the theoretical curve as shown in Fig. 12 results. The order of magnitude and shape agree with test except at the higher explosion chamber pressures. The concept of such a total pressure might be imagined by considering two opposing air flows stagnating on an object anchored in the stream.

The increase in P_t in going from the downstream to the upstream station is physically understandable due to the fact that it is associated with a supersonic flow of velocity w_1 relative to the tube flow. In going into a smaller area, it in effect is being supersonically diffused with a corresponding pressure increase.

It is to be concluded that this method of introducing a shock wave into moving air is practical and effective. However, due to the flattening P_2/P_1 upstream characteristic shown in Fig. 13, little pressure ratio would be gained by increasing the explosion chamber pressure past values used in this experimentation.

CONCLUSIONS AND RECOMMENDATIONS

As a result of the tests conducted with medium pressure disturbances moving into high subsonic air flow, it is concluded that strain gages provide a versatile pressure pickup element with ease of use dictated by the amplifier-recording equipment despite the preference of many investigators for quartz crystal pickups.

Introduction of pressure disturbances at right angles to the air flow by rupture of a diaphragm is a satisfactory method for explosion chamber pressures of between 35 and 85 psig. Additional pressure would give but little increase to the pressure ratio across the disturbance wave or to its velocity

By theory and comparison with results from the shock tube, the pressure ratio data taken at the shock end of the flow tube is invalidated due to the proximity of the pressure pickup to the shock inlet and not due to any limitation of the strain gage pickup. A pressure measurement station must be sufficiently removed from the shock inlet to allow formation of the pressure wave it is desired to observe.

The validity of superimposing an initial flow on the velocity of a wave from a shock tube is substantiated within the limits of the measuring techniques used. The absolute velocity of such a wave propagating into moving air is a function of the pressure ratio across the disturbance, tube flow velocity, and the two energy levels represented by the total temperature of the tube flow and the total temperature of the explosion chamber.

Altho non-existent in shock tube experiments, the propagation

of a shock disturbance into moving air produced a peak of pressure within the disturbance of considerably greater magnitude than the pressure P_2 immediately behind the shock. A qualitative method of calculating this peak is indicated possible by considering such a pressure to be the static pressure associated with accelerating a flow from rest at a total pressure P_0 to a velocity w with respect to the normal tube flow. Furthermore, it is indicated that this peak pressure is diffused by moving upstream into a reduced area region at a supersonic velocity relative to the tube flow.

A new parameter which is of considerable use is introduced and defined as $N = \frac{w}{\sqrt{g \sigma RT_0}}$, the ratio of shock velocity relative to the flow into which it is going to the energy of the gas expressed in terms of the absolute total temperature of the flow.

It is recommended that this study be continued specifically with the aim of propagating pressure disturbances into flow of constant Mach number to observe any attenuation tendencies and to more closely determine the velocity of wave propagation. In such an effort, more than two stations along the flow path should be instrumented, and a more time-responsive unit such as a multichannel oscilloscope with camera recording used to observe results.

A further interesting variation would be to propagate the waves into slightly supersonic flow.

It is also suggested that a more comprehensive mathematical analysis be tried, starting with the physical situation as it exists rather than relying on superposition.

REFERENCES

- (A). Bailey, N. P.: THE THERMODYNAMICS OF AIR AT HIGH VELOCITIES.
Journal of the Aeronautical Sciences, Vol. 11, No. 3. July 1944.
- (P). Timoshenko, S.: STRENGTH OF MATERIALS, VOLUMES I & II. 1940.
2nd ed. Van Nostrand Co., Inc., New York.
- (C). Timoshenko, S.: VIBRATION PROBLEMS IN ENGINEERING. 1937.
2nd ed. Van Nostrand Co., Inc., New York.
- (D). Geiger, F. W. and Mautz, C. W.: THE SHOCK TUBE AS AN INSTRUMENT
FOR THE INVESTIGATION OF TRANSONIC AND SUPERSONIC FLOW PATTERNS.
June 1949. Published by the University of Michigan for the
Office of Naval Research under Contract N6-ONR-332.
- (E). Elsakney, W. and Taub, A. H.: INTERACTION OF SHOCK WAVES.
Reviews of Modern Physics, Vol. 21, No. 4. October 1949.

APPENDIX IFLOW TUBE DESIGN CONSIDERATIONS

From Ref. (A), for a diffuser or nozzle with friction, the expression for velocity gradient is developed and given as

$$\frac{dv}{dx} = v \left[\frac{\frac{f \gamma M^2}{2m} - \frac{1}{A} \frac{dA}{dx}}{1 - M^2} \right]$$

Since

$$\frac{v}{\sqrt{\gamma R T_0}} = \frac{M}{\sqrt{1 + \frac{\gamma-1}{2} M^2}}$$

a tube under steady flow conditions at constant Mach number will have a constant velocity. Then $\frac{dv}{dx} = 0$ and

$$\frac{f \gamma M^2}{2m} = \frac{1}{A} \frac{dA}{dx}$$

or

$$\frac{f \gamma M^2}{2} = \frac{m}{A} \frac{dA}{dx}$$

For a tube of rectangular cross section with equal wall angles (α);

$$\frac{m}{A} \frac{dA}{dx} = \tan \alpha = \text{Constant}$$

$$\frac{f \gamma M^2}{2} = \tan \alpha$$

Design for conditions:

$$M = 0.8 \quad \frac{W \sqrt{T_0}}{A P} = .7788$$

$$f = .007 \text{ (assumed)}$$

$$W_{\max} = 0.49 \text{ lbs/sec from two Shram compressors.}$$

$$T_0 = 95^\circ \text{ F} = 555^\circ \text{ R.}$$

$$\text{Tube length} = 32 \text{ inches.}$$

Exit conditions:

$$P_{\text{exit}} = 14.7 \text{ psia.}$$

$$\text{Max. } A_{\text{exit}} = \frac{W\sqrt{T_0}}{.7788 P_{\text{ex}}} = \frac{(.49)\sqrt{555}}{.7788 (14.7)} = 1.006 \text{ in}^2$$

$$\tan \alpha = \frac{(.007)(1.395)(0.8)^2}{2} = .00312$$

Specify: ,

$$A_{\text{exit}} = 0.9 \times 1.1 \text{ in.} = .99 \text{ in}^2$$

The decrease per side of the rectangular cross section on going from exit to throat is $2L \tan \alpha = .20 \text{ in.}$ Dimensions of the cross section at the throat are then $0.7 \times 0.9 \text{ in.} = 0.63 \text{ in}^2$.

$$W = \frac{.7788(.99)(14.7)}{\sqrt{555}} = .482 \frac{\text{lb}}{\text{sec.}}$$

Construction of the tube is facilitated by using a single taper instead of the double taper. If the throat and exit areas as computed are maintained

$$\text{Throat} \quad 0.7 \times 0.9 \text{ in.} = 0.63 \text{ in}^2$$

$$\text{Exit} \quad 1.1 \times 0.9 \text{ in.} = 0.99 \text{ in}^2$$

by using a single taper, the maximum deviation in area from the double taper is 1.3% occurring at the center of the tube. One pair of tube walls then has a constant inside dimension of 0.9 in. The other pair tapers from 0.7 in. at the throat to 1.1 in. at the exit.

Static pressure taps located at 2, 10, 18, and 26 inches from the throat have corresponding cross sectional areas:

$$\text{At } 2 \text{ in.} \quad 0.9 \times 0.725 \text{ in.} = 0.6525 \text{ in}^2.$$

$$10 \text{ in.} \quad 0.9 \times 0.825 \text{ in.} = 0.7425 \text{ in}^2.$$

$$18 \text{ in.} \quad 0.9 \times 0.925 \text{ in.} = 0.8325 \text{ in}^2.$$

$$26 \text{ in.} \quad 0.9 \times 1.025 \text{ in.} = 0.9225 \text{ in}^2.$$

APPENDIX II

FLUSH-MOUNTED PRESSURE PICKUP DESIGN AND ANALYSISDesign limitations:

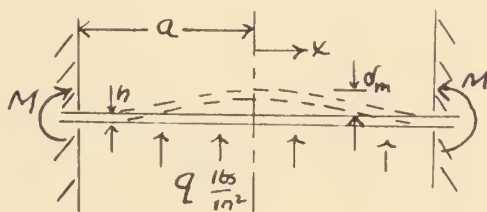
Circular diaphragm of radius 9/32 inch.

Maximum diaphragm strain of 600 microinches/inch at the center as dictated by material and strain gage amplification equipment.

Strain gage mounted at the center.

Maximum pressure of 100 psig but good response desired for pressures as low as five psig.

From Ref.(B), consider the diaphragm as a plate with clamped edges.



h = diaphragm thickness

σ_m = Deflection at center

M = bending moment at edge

σ = stress

μ = Poisson's ratio

ϵ = strain

E = modulus of elasticity

For a disc with clamped edges:

$$\sigma_{x=0} = \frac{6}{h^2} M_{x=0}$$

$$M_{x=0} = \left(\frac{1+\mu}{16}\right) q a^2$$

$$\sigma_{x=0} = \sigma_{y=0} = \frac{6}{h^2} \left(\frac{1+\mu}{16}\right) q a^2$$

As an approximation, consider the center of the diaphragm to be essentially flat and stressed by simple tensile stress. Then

$$\begin{aligned}\epsilon_{x=0} &= \frac{\sigma_{x=0} - \mu \sigma_{y=0}}{E} = \frac{\sigma_{x=0} (1-\mu)}{E} \\ &= \frac{6}{h^2} \left(\frac{1+\mu}{16} \right) q a^2 \frac{(1-\mu)}{E} \\ \epsilon_{x=0} &= \frac{3}{8} \frac{(1-\mu^2)}{E} \frac{q a^2}{h^2} \times 10^6 \frac{\text{micro in.}}{\text{in.}}\end{aligned}$$

For:

Material: Brass.

E = 14×10^6 psi.

$\mu = .3$

a = .281 in.

h = .020 in.

$$\sigma_{x=0} = 96.2 q \frac{\text{lbs}}{\text{in}^2}$$

$$\epsilon_{x=0} = 4.81 q \frac{\text{micro in.}}{\text{in.}}$$

To see the effects of a low pressure of five psi and a high pressure of 100 psi:

q psi	5	100
$\sigma_{x=0}$	481	9620
$\epsilon_{x=0}$	24	481

These strain limits could be covered with one gage voltage and attenuator setting for use with A-8 type strain gages and the Hathaway strain gage amplifier and oscillograph. Stress values are indicated within elastic limits for brass.

Frequency analysis:

From Ref. (C), the natural frequency of a circular disc rigidly clamped at the edge is given,

$$P = \frac{\alpha}{2\pi a^2} \frac{1}{\sqrt{1+\beta}} \sqrt{\frac{gD}{\delta h}} \sqrt{1 + 1.464 \frac{a_1^2}{h^2}}$$

$\alpha = 10.21$ for lowest mode of vibration.

$a^2 = .079$ in². Radius squared.

$\beta = 0$. Correction for differences in fluid density.

$g = 32.2$ ft/sec². Gravitational constant.

$D = 10.24$ lb-in. = $Eh^3/12(1-\mu^2)$.

$\delta = 534$ lb/ft³. Wt. per unit volume of diaphragm material.

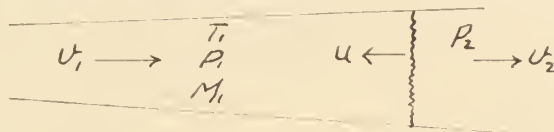
$h = .020$ in. Thickness.

$a_1 = .000476$ in. = $qa^4/64D$. Deflection at center for 50 psig load.

With these values, the natural frequency is calculated to be 16,460 cycles per second.

APPENDIX III

DERIVATION OF THE PRESSURE WAVE VELOCITY EQUATION



For the assumed condition of flow of constant Mach number thru the tube prior to the introduction of the pressure wave, v_1 , T_1 , T_0 , and P_1 are also constant.

The disturbance in going upstream with absolute velocity u moves with velocity w relative to the tube flow velocity. For a stationary disturbance, w would represent the tube flow velocity ahead of the disturbance. For a disturbance moving into a stationary gas, w would be the velocity of the disturbance.

In writing the idealized equations, the disturbance is assumed to have no thickness so that flow passes thru the disturbance at constant flow area. Also, it may be rationalized that the increase in tube area from the throat, determined in Appendix I as necessary to hold constant Mach number, is needed only because of friction. With the elimination of friction from the equations, area change is also eliminated.

$$\text{Continuity:} \quad \rho_1 w_1 = \rho_2 w_2 \quad (1)$$

$$\text{Momentum:} \quad P_1 + \rho_1 w_1^2 = P_2 + \rho_2 w_2^2 \quad (2)$$

$$\text{Energy:} \quad dL + dQ = C_p dT + \frac{1}{Jg} w dw \quad (3)$$

from which

$$C_p T_1 + \frac{1}{Jg} \frac{w_1^2}{2} = C_p T_2 + \frac{1}{Jg} \frac{w_2^2}{2}$$

$$C_p = \frac{\gamma}{\gamma-1} \frac{R}{J}$$



$$w_1^2 + \frac{2\gamma}{\gamma-1} Rg T_1 = w_2^2 + \frac{2\gamma}{\gamma-1} Rg T_2$$

$$w_1^2 + \frac{2\gamma}{\gamma-1} \frac{P_1}{\rho_1} = w_2^2 + \frac{2\gamma}{\gamma-1} \frac{P_2}{\rho_2} \quad (4)$$

Divide Eq. (2) by (1):

$$\frac{P_1}{\rho_1 w_1} + w_1 = \frac{P_2}{\rho_2 w_2} + w_2 \quad (5)$$

from which

$$w_1 - w_2 = \frac{P_2}{\rho_2 w_2} - \frac{P_1}{\rho_1 w_1} \quad (6)$$

Multiply thru by $(w_1 + w_2)$:

$$w_1^2 - w_2^2 = (w_1 + w_2) \left[\frac{P_2}{\rho_2 w_2} - \frac{P_1}{\rho_1 w_1} \right] \quad (7)$$

Combine this with the energy Eq. (4):

$$(w_1 + w_2) \left[\frac{P_2}{\rho_2 w_2} - \frac{P_1}{\rho_1 w_1} \right] = \frac{2\gamma}{\gamma-1} \left[\frac{P_2}{\rho_2} - \frac{P_1}{\rho_1} \right] \quad (8)$$

From Eq. (1):

$$w_2 = \frac{\rho_1 w_1}{\rho_2}$$

Eq. (8) becomes:

$$\left[\frac{\rho_1 w_1}{\rho_1} + \frac{\rho_1 w_1}{\rho_2} \right] \left[\frac{P_2}{\rho_1 w_1} - \frac{P_1}{\rho_1 w_1} \right] = \frac{2\gamma}{\gamma-1} \left[\frac{P_2}{\rho_2} - \frac{P_1}{\rho_1} \right] \quad (9)$$

$$\frac{P_2}{\rho_1} - \frac{P_1}{\rho_1} + \frac{P_2}{\rho_2} - \frac{P_1}{\rho_2} = \frac{2\gamma}{\gamma-1} \left[\frac{P_2}{\rho_2} - \frac{P_1}{\rho_1} \right] \quad (10)$$

$$\frac{1}{\rho_1} \left[P_2 - P_1 + \frac{2\gamma}{\gamma-1} P_1 \right] = \frac{1}{\rho_2} \left[P_1 - P_2 + \frac{2\gamma}{\gamma-1} P_2 \right] \quad (11)$$

$$\frac{P_2}{\rho_1} = \frac{w_1}{w_2} = \frac{P_1 + P_2 \left(\frac{2\gamma}{\gamma-1} - 1 \right)}{P_2 + P_1 \left(\frac{2\gamma}{\gamma-1} - 1 \right)} = \frac{P_1 + P_2 \left(\frac{\gamma+1}{\gamma-1} \right)}{P_2 + P_1 \left(\frac{\gamma+1}{\gamma-1} \right)} \quad (12)$$

This is the Rankine-Hugoniot Equation relating velocities and pressures on either side of a normal shock front.

From Eq. (3):

$$c_p \int_{T_0}^T dT + \frac{1}{\gamma} \int_0^w w dw = 0 \quad (13)$$

$$\frac{w_1^2}{2\gamma} = c_p (T_0 - T_1)$$



$$\omega_1^2 = 2gR \frac{\sigma}{\sigma-1} (\bar{T}_0 - \bar{T}_1) \quad (14)$$

$$\begin{aligned} \omega_1^2 + \frac{2\sigma}{\sigma-1} \frac{P_1}{\rho_1} &= 2gR \frac{\sigma}{\sigma-1} (\bar{T}_0 - \bar{T}_1) + \frac{2\sigma}{\sigma-1} gR \bar{T}_1 \\ &= \frac{2}{\sigma-1} g\sigma R \bar{T}_0 \end{aligned}$$

$$\frac{\sigma}{\sigma-1} \frac{P_1}{\rho_1} = \frac{1}{\sigma-1} g\sigma R \bar{T}_0 - \frac{1}{2} \omega_1^2 \quad (15)$$

Also

$$\frac{\sigma}{\sigma-1} \frac{P_2}{\rho_2} = \frac{1}{\sigma-1} g\sigma R \bar{T}_0 - \frac{1}{2} \omega_2^2 \quad (16)$$

From Eq. (15) and (16):

$$P_1 = \rho_1 \left[\frac{g\sigma R \bar{T}_0}{\sigma} - \frac{\sigma-1}{2\sigma} \omega_1^2 \right] \quad (17)$$

$$P_2 = \rho_2 \left[\frac{g\sigma R \bar{T}_0}{\sigma} - \frac{\sigma-1}{2\sigma} \omega_2^2 \right] \quad (18)$$

Substituting these expressions in Eq. (2):

$$\rho_1 \left[\frac{2}{\sigma+1} g\sigma R \bar{T}_0 + \omega_1^2 \right] = \rho_2 \left[\frac{2}{\sigma+1} g\sigma R \bar{T}_0 + \omega_2^2 \right] \quad (19)$$

Then from continuity, Eq. (1):

$$\begin{aligned} \omega_1 \rho_1 &= \omega_2 \rho_2 \\ &= \rho_1 \left[\frac{\frac{2}{\sigma+1} g\sigma R \bar{T}_0 + \omega_1^2}{\frac{2}{\sigma+1} g\sigma R \bar{T}_0 + \omega_2^2} \right] \omega_2 \end{aligned} \quad (20)$$

$$\frac{2}{\sigma+1} g\sigma R \bar{T}_0 [\omega_1 - \omega_2] = -\omega_1 \omega_2^2 + \omega_2 \omega_1^2 \quad (21)$$

$$\frac{2}{\sigma+1} g\sigma R \bar{T}_0 = \frac{\omega_2 \omega_1^2 - \omega_1 \omega_2^2}{\omega_1 - \omega_2} \quad (22)$$

$$\frac{2}{\sigma+1} g\sigma R \bar{T}_0 = \omega_1 \omega_2 \quad (23)$$

This is the Prandtl Relation correlating flow velocity ahead of and behind a normal shock.

Development to here was adapted from Ref's. (A) and (D).



For the case under consideration, the disturbance is moving at absolute velocity u into a flow of velocity v . T_0' now refers to the total temperature associated with velocity w_1 .

$$|u| = |w_1| - |v|$$

or
$$w_1 = u + v \quad (24)$$

From Eq. (23) and (12):

$$w_2 = \frac{1}{w_1} \frac{2}{\gamma+1} \gamma \gamma R T_0' \quad (25)$$

$$w_1 = w_2 \left[\frac{1 + \frac{\gamma+1}{\gamma-1} \frac{P_2}{P_1}}{\frac{P_2}{P_1} + \frac{\gamma+1}{\gamma-1}} \right] \quad (26)$$

Substituting (25) in (26):

$$w_1^2 = \frac{2}{\gamma+1} \gamma \gamma R T_0' \left[\frac{1 + \frac{\gamma+1}{\gamma-1} \frac{P_2}{P_1}}{\frac{P_2}{P_1} + \frac{\gamma+1}{\gamma-1}} \right] \quad (27)$$

or

$$(u+v)^2 = \gamma \gamma R T_0' \frac{2}{\gamma+1} \left[\frac{1 + \frac{\gamma+1}{\gamma-1} \frac{P_2}{P_1}}{\frac{P_2}{P_1} + \frac{\gamma+1}{\gamma-1}} \right] \quad (28)$$

It is desired to get an expression for the velocity ratio, $\frac{u}{\sqrt{\gamma \gamma R T_0}}$ since T_0 remains constant while T_0' varies with the explosion chamber pressure. With the air in the explosion chamber coming from the same source as air in the flow tube, their temperatures and pressures are linked ideally thru the adiabatic relation

$$\frac{T_0'}{T_0} = \left(\frac{P_2}{P_0} \right)^{\frac{\gamma-1}{\gamma}} \quad (29)$$

Then

$$(u+v)^2 = \gamma \gamma R T_0 \left(\frac{P_2}{P_0} \right)^{\frac{\gamma-1}{\gamma}} \frac{2}{\gamma+1} \left[\frac{1 + \frac{\gamma+1}{\gamma-1} \frac{P_2}{P_1}}{\frac{P_2}{P_1} + \frac{\gamma+1}{\gamma-1}} \right] \quad (30)$$



$$\frac{U}{\sqrt{g\delta RT_0}} = \left(\frac{P_0}{P_1}\right)^{\frac{\delta-1}{2\delta}} \sqrt{\frac{2}{\delta+1} \left[\frac{1 + \frac{\delta+1}{\delta-1} \frac{P_2}{P_1}}{\frac{P_2}{P_1} + \frac{\delta+1}{\delta-1}} \right]} = M_1 \sqrt{\frac{1}{1 + \frac{\delta-1}{2} M_1^2}} \quad (31)$$

Consider the shock moving with speed w_1 into still air. Then converting T_0' to T_1 by

$$\frac{T_0'}{T_1} = 1 + \frac{\delta-1}{2} \frac{w_1^2}{g\delta RT_1} \quad (32)$$

Eq. (27) becomes

$$w_1^2 = g\delta RT_1 \left[1 + \frac{\delta-1}{2} \frac{w_1^2}{g\delta RT_1} \right] \frac{2}{\delta+1} \left[\frac{1 + \frac{\delta+1}{\delta-1} \frac{P_2}{P_1}}{\frac{P_2}{P_1} + \frac{\delta+1}{\delta-1}} \right] \quad (33)$$

$$\frac{w_1^2}{g\delta RT_1} = \frac{\frac{2}{\delta+1} \left[1 + \frac{\delta+1}{\delta-1} \frac{P_2}{P_1} \right]}{\frac{\delta+1}{\delta-1} - \frac{\delta-1}{\delta+1}}$$

$$\frac{w_1^2}{g\delta RT_1} = \frac{(\delta+1) \frac{P_2}{P_1} + (\delta-1)}{2\delta} \quad (34)$$



TABLE I
FLOW TUBE CALIBRATION DATA

		Without exit Receiver Chamber	With exit Receiver Chamber
Plenum Chamber Data	Chamber psig	32	22
	Barom. psia	14.7	14.58
	Total Press. P_o	36.7	36.58
	T_o	563	559
Metering Nozzle Data	ΔP mm "Hg	11.0	11.0
	ΔP psi	5.41	5.41
	P_{inlet} psia	42.71	41.99
	P_i/P_o	1.148	1.148
	M_{nozzle}	.450	.450
	$\frac{w\sqrt{\gamma}}{AP}$.421	.421
	W lbs/sec	.508	.511
2" Station $A = .6525$	"Hg gage	+0.7	+11.2
	P psia	15.0	20.09
	$\frac{w\sqrt{\gamma}}{AP}$	1.220	.921
	M	1.179	.938
10" Station $A = .7425$	"Hg gage	-2.6	+15.0
	P psia	13.4	21.96
	$\frac{w\sqrt{\gamma}}{AP}$	1.200	.740
	M	1.162	.764
18" Station $A = .8325$	"Hg gage	-5.1	+16.6
	P psia	12.2	22.75
	$\frac{w\sqrt{\gamma}}{AP}$	1.177	.636
	M	1.143	.665
26" Station $A = .9225$	"Hg gage	+4.2	+18.2
	P psia	16.8	23.53
	$\frac{w\sqrt{\gamma}}{AP}$.772	.557
	M	.794	.588

TABLE II

LABORATORY TEST DATA FROM OSCILLOGRAPHS
(Arranged in order of increasing P_e)

1	2	3	4	5	6	7	8	9	10	11	12
Run	Date	Barom. " Hg	P_{gage}	P_{corr} PSIG	P_{oflow} psia	T_o °R	P_t in. defl.	P_t psi	P_2 in. defl.	P_2 psi	Δt sec.
DYNAMIC GAGE AT UPSTREAM (2") STATION											
2	4-14	29.64	35	33.4	36.53	565	.24	15.9	.19	12.6	.00437
12	4-16	29.89	41	39.3	36.67	559	.31	20.5	.22	14.6	.00370
6	4-14	29.64	45	43.2	36.53	544	.33	21.9	.22	14.6	.00353
3	4-14	29.64	54	52.0	36.53	554	.30	19.9	.21	13.9	.00373
13	4-16	29.89	55	53.0	36.67	558	.38	25.4	.24	15.9	.00305
7	4-14	29.64	65	62.7	36.53	557	.42	27.9	.24	15.9	.00311
4	4-14	29.64	75	72.5	36.53	549	.44	29.2	.24	15.9	.00304
1	4-14	29.64	82	79.3	36.53	562	.44	29.2	.24	15.9	.00289
5	4-14	29.64	88	85.2	36.53	548	.45	29.9	.25	16.6	.00304
DYNAMIC GAGE AT DOWNSTREAM (26") STATION											
8	4-14	29.64	35	33.4	36.53	548	.21	13.9	.21	13.9	.00420
10	4-14	29.64	50	48.1	36.53	544	.29	18.6	.29	18.6	.00319
14	4-21	30.42	60	57.7	36.92	549	.30	19.9	.30	19.9	.00298
11	4-14	29.64	70	67.6	36.53	549	.32	21.3	.32	21.3	.00269
15	4-21	30.42	77	74.4	36.92	548	.34	22.5	.34	22.5	.00268
9	4-14	29.64	86	83.2	36.53	546	.36	23.9	.36	23.9	.00264

P_t and P_2 are psi above P , at measuring station.



TABLE III

TEST DATA

(Corrected to 14.7 psia atmosphere; T_{flow} 552°R.)

1	2	3	4	5	6	7	8	9
Run	P _{e corr} psig	P _t psig	P _t psia	P ₂ psig	P ₂ psia	$\frac{P_2}{P_1}$	u ft/sec	$\frac{u}{\sqrt{g \theta RT}}$
DYNAMIC GAGE AT UPSTREAM (2") STATION								
2	33.4	21.4	36.1	18.1	32.8	1.622	457	.397
12	39.3	26.0	40.7	20.1	34.8	1.722	540	.469
6	43.2	27.4	42.1	20.1	34.8	1.722	567	.492
3	52.0	25.4	40.1	19.4	34.1	1.689	536	.466
13	53.0	30.9	45.6	21.4	36.1	1.788	656	.569
7	62.7	33.4	48.1	21.4	36.1	1.788	643	.558
4	72.5	34.7	49.4	21.4	36.1	1.788	658	.572
1	79.3	34.7	49.4	21.4	36.1	1.788	692	.601
5	85.2	35.4	50.1	22.1	36.8	1.822	658	.572
DYNAMIC GAGE AT DOWNSTREAM (26") STATION								
8	33.4	22.9	37.6	22.9	37.6	1.592	477	.413
10	48.1	27.6	42.3	27.6	42.3	1.790	627	.543
14	57.7	28.9	43.6	28.9	43.6	1.843	671	.582
11	67.6	30.3	45.0	30.3	45.0	1.904	743	.644
15	74.4	31.5	46.2	31.5	46.2	1.954	747	.648
9	83.2	32.9	47.6	32.9	47.6	2.010	757	.657

At upstream station: P₁ = 5.51 psig = 20.21 psia.At downstream station: P₂ = 8.95 psig = 23.65 psia.



TABLE IV

PRESSURE RATIO, SPEED RATIO DATA
FROM PAIRED TEST CURVES

1	2	3	4	5
Run	P _e corr psia	$\frac{P_2}{P_1}$	Δt sec	$\frac{u}{\sqrt{g \gamma R T_0}}$
UPSTREAM (3") STATION				
2	48.1	1.610	.00427	.407
12	54.0	1.696	.00370	.469
6	57.9	1.737	.00348	.498
3	66.7	1.682	.00378	.458
13	67.7	1.734	.00305	.568
7	77.4	1.798	.00293	.592
4	87.2	1.802	.00387	.604
1	94.0	1.803	.00385	.608
5	99.9	1.805	.00383	.612
DOWNSTREAM (.26") STATION				
8	48.1	1.610	.00427	.407
10	62.8	1.790	.00322	.538
14	72.4	1.851	.00299	.582
11	82.3	1.907	.00389	.600
15	89.1	1.942	.00386	.607
9	97.9	1.988	.00284	.611

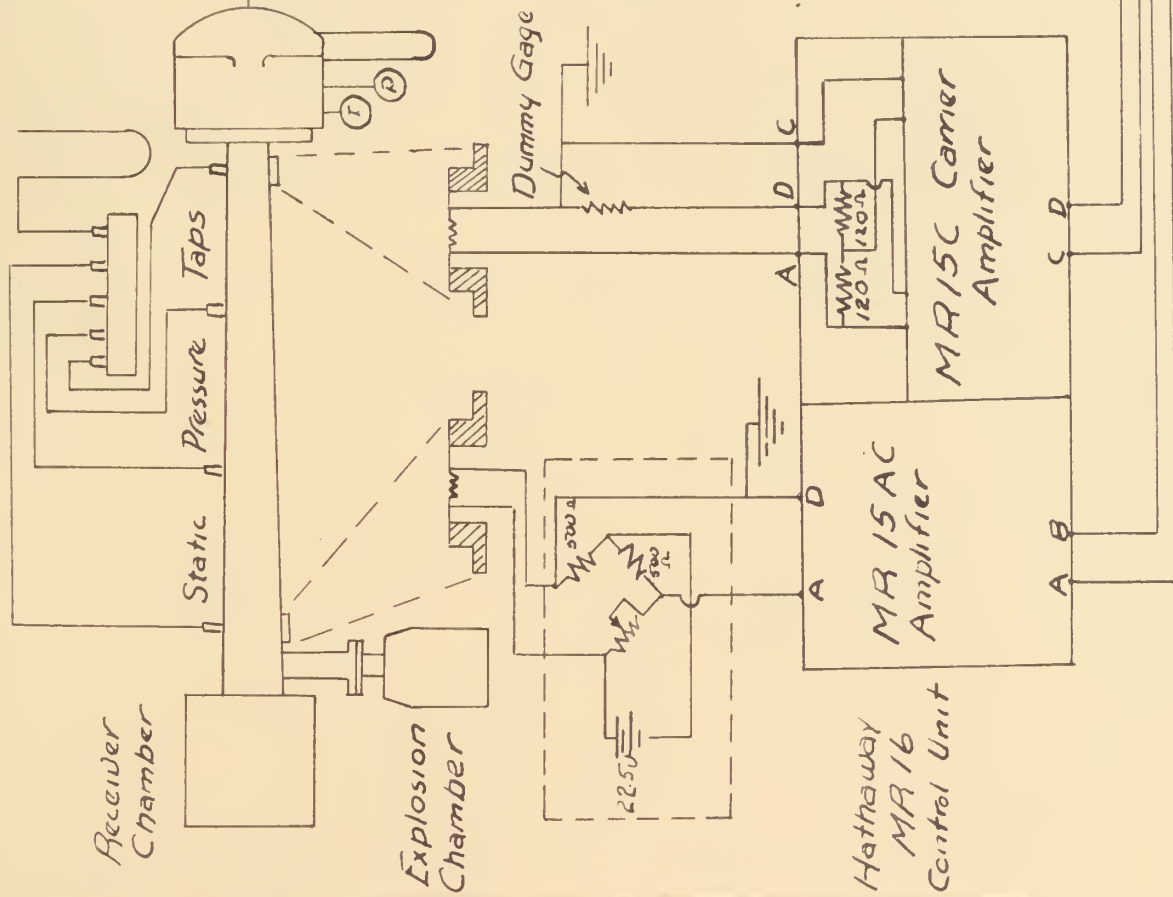


FIG. 1
SCHEMATIC OF
ARRANGEMENT OF
LABORATORY TEST
SETUP.



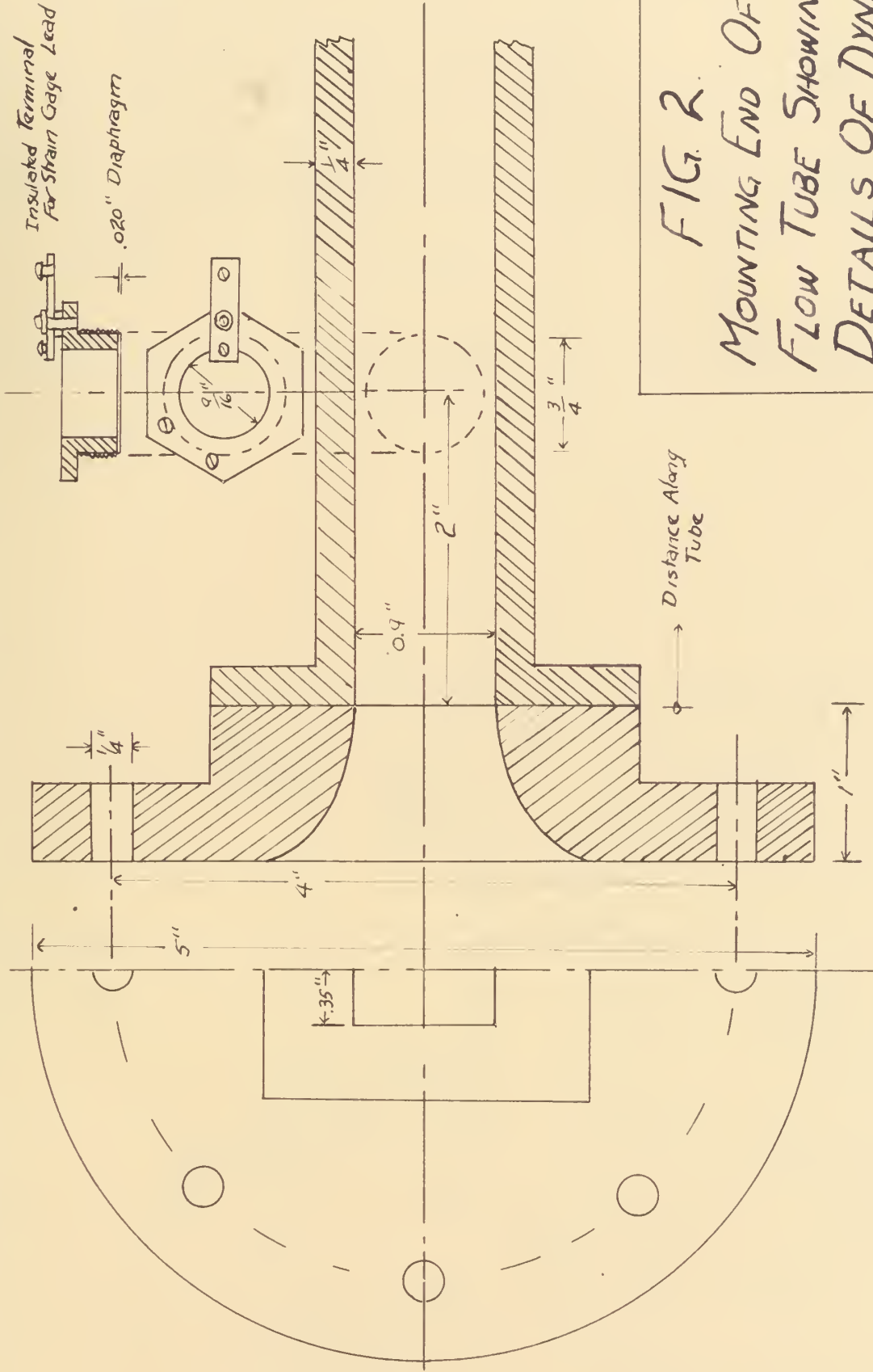


FIG. 2.
MOUNTING END OF
FLOW TUBE SHOWING
DETAILS OF DYNAMIC
PRESSURE PICKUP



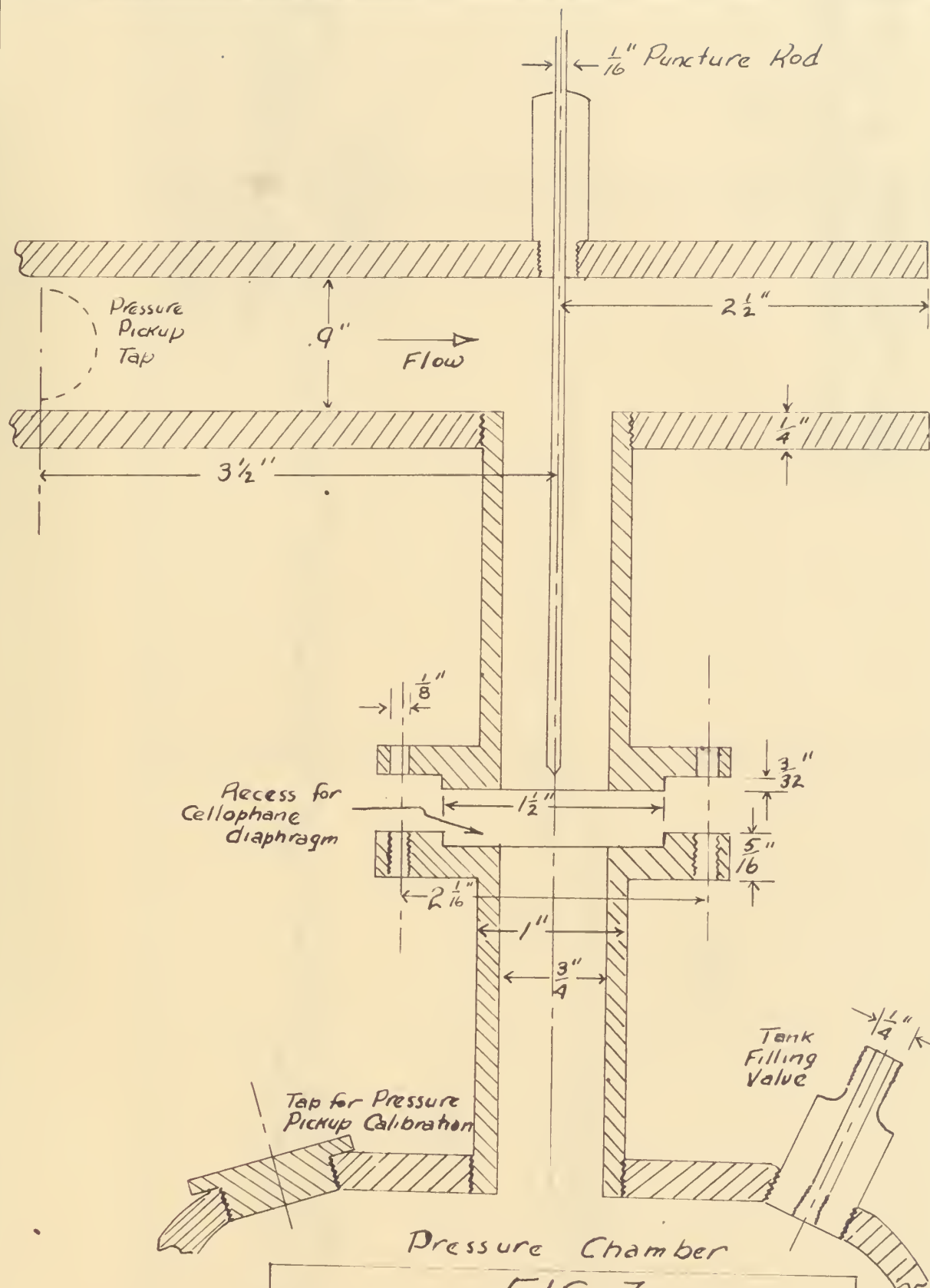


FIG. 3.
EXIT END OF FLOW TUBE
SHOWING SHOCK
PRODUCTION ARRANGEMENT.



Run 13

4-16-51

Barom. 29.87

$P_2 = 53.0$ (corrected) psig

$P_1 = 5.51$ psig

$I_{12} = 66.8$ psig

Downstream Face

(For time only)

→ Time

Δt

P_2

P_1

Upstream Trace

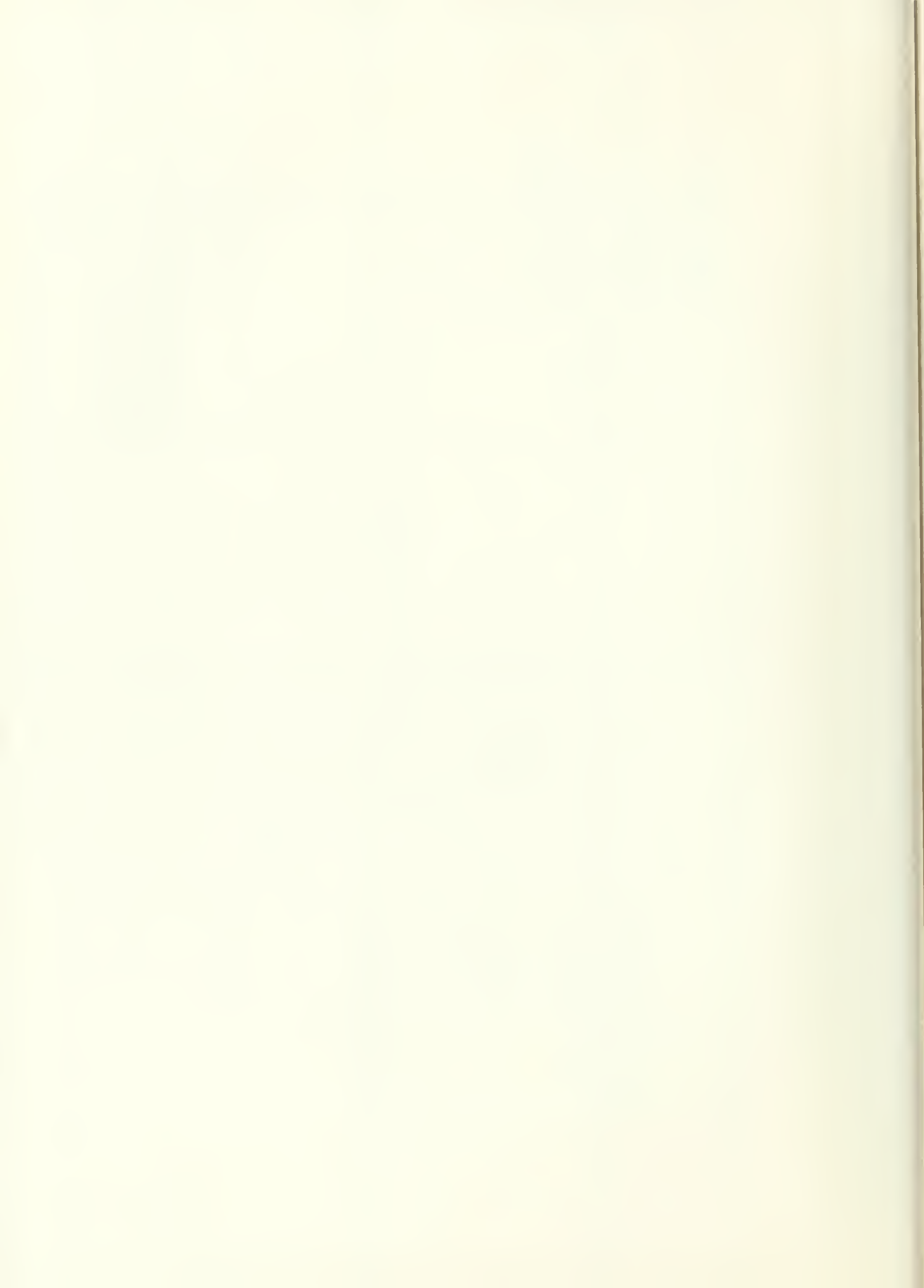
P

→ .01 sec

FIG. 4.

OSCILLOGRAPH WITH DYNAMIC
PRESSURE GAGE AT UPSTREAM

END.



Run 15
4-21-51
Barom 30.4"
 $P_c = 74.4 \text{ psig (corrected)}$
 $P = 8.95 \text{ psig}$

Upstream Face

Time →

Δt

P_c — P_i

Downstream Trace

F/G. 5

OSCILLOGRAPHY WITH DYNAMIC
PRESSURE GAGE AT SHOCK
(DOWNSTREAM) END.

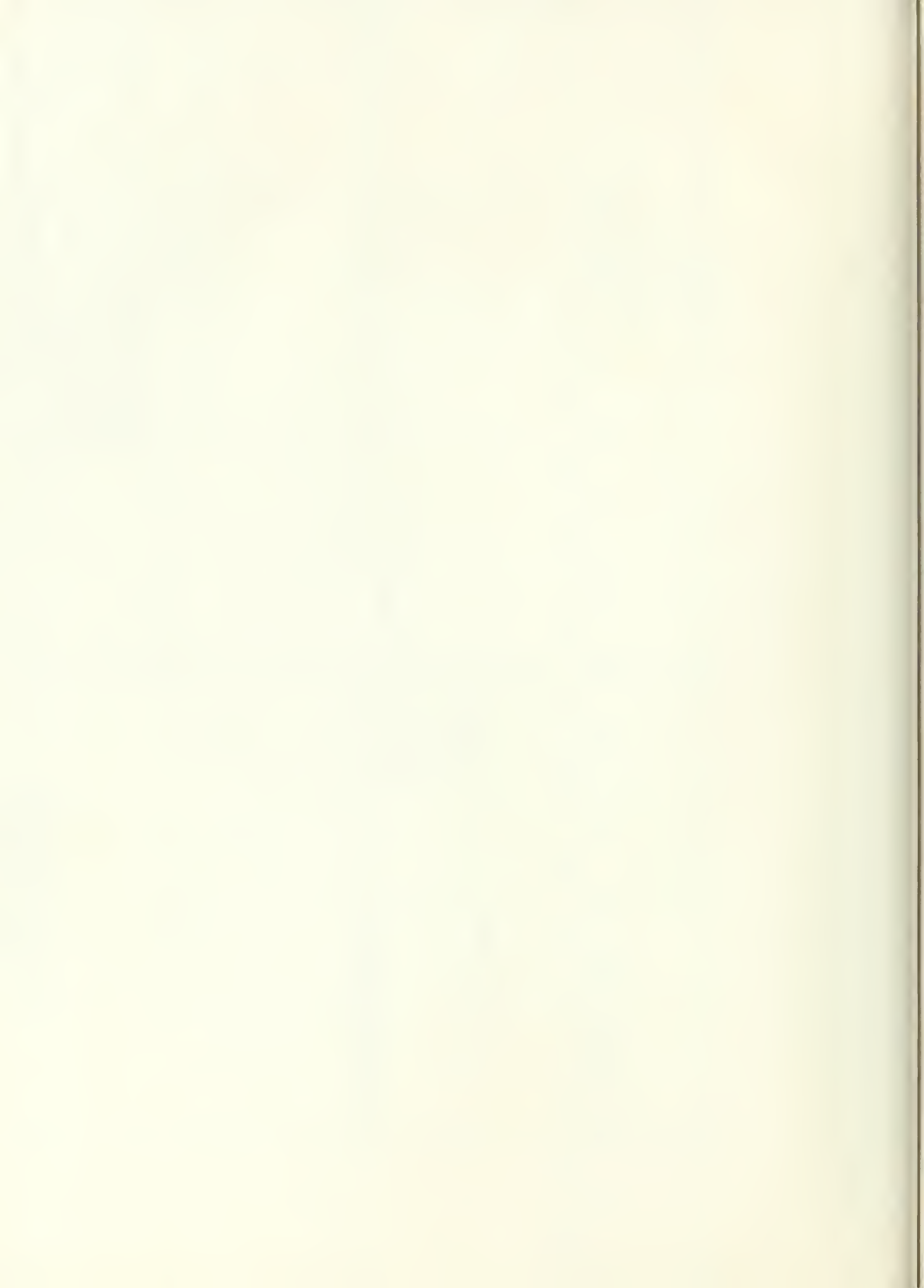


FIG. 6

GENERAL VIEW OF TEST SETUP

At the left is the lathe bed which supports the plenum chamber to which is bolted the flow tube. On the table to the left is the Hathaway S-14A oscillograph with the MRC 16 control unit to the right. Small metal box between houses the external bridge circuit with lead to the pressure sensing element.

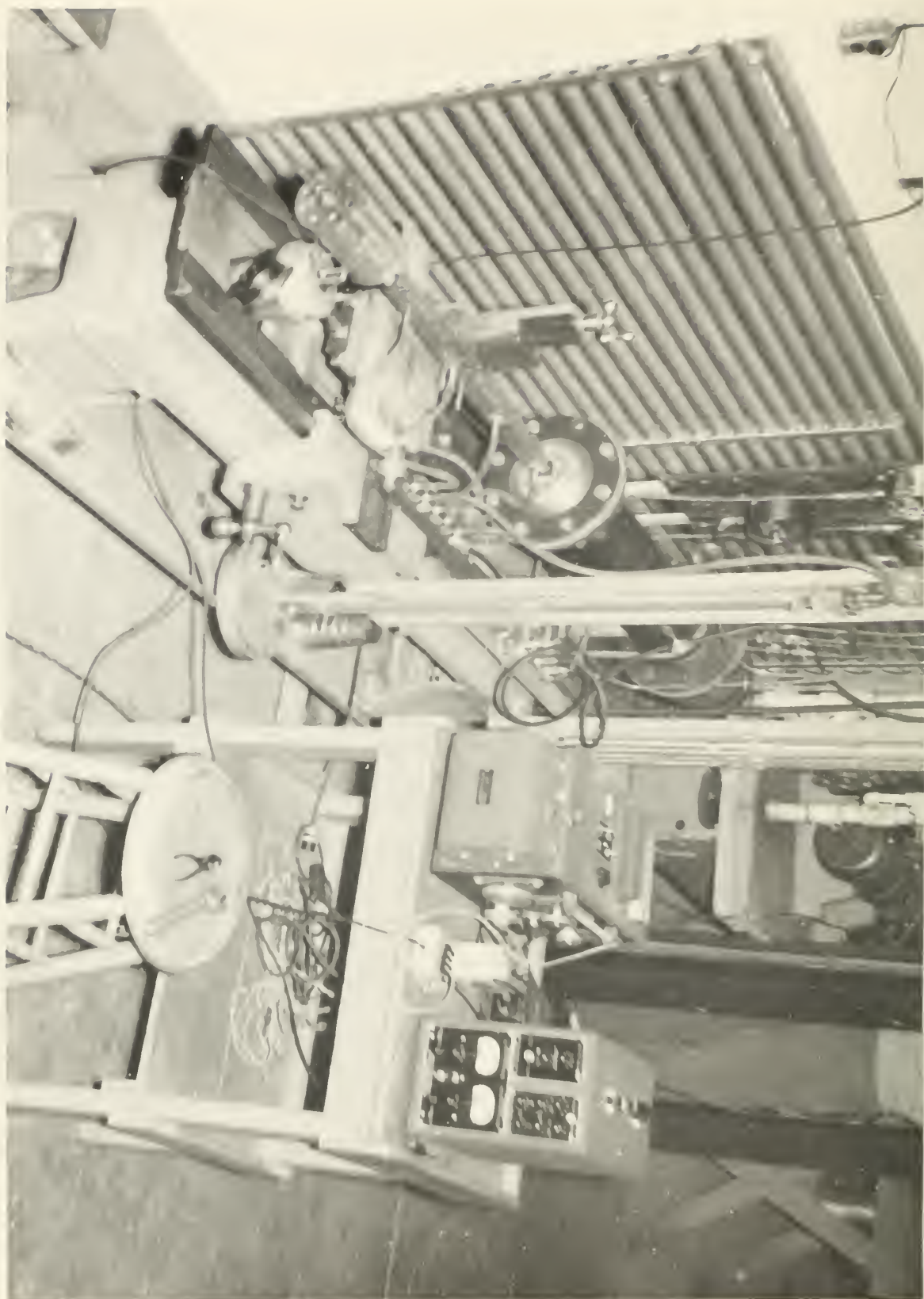
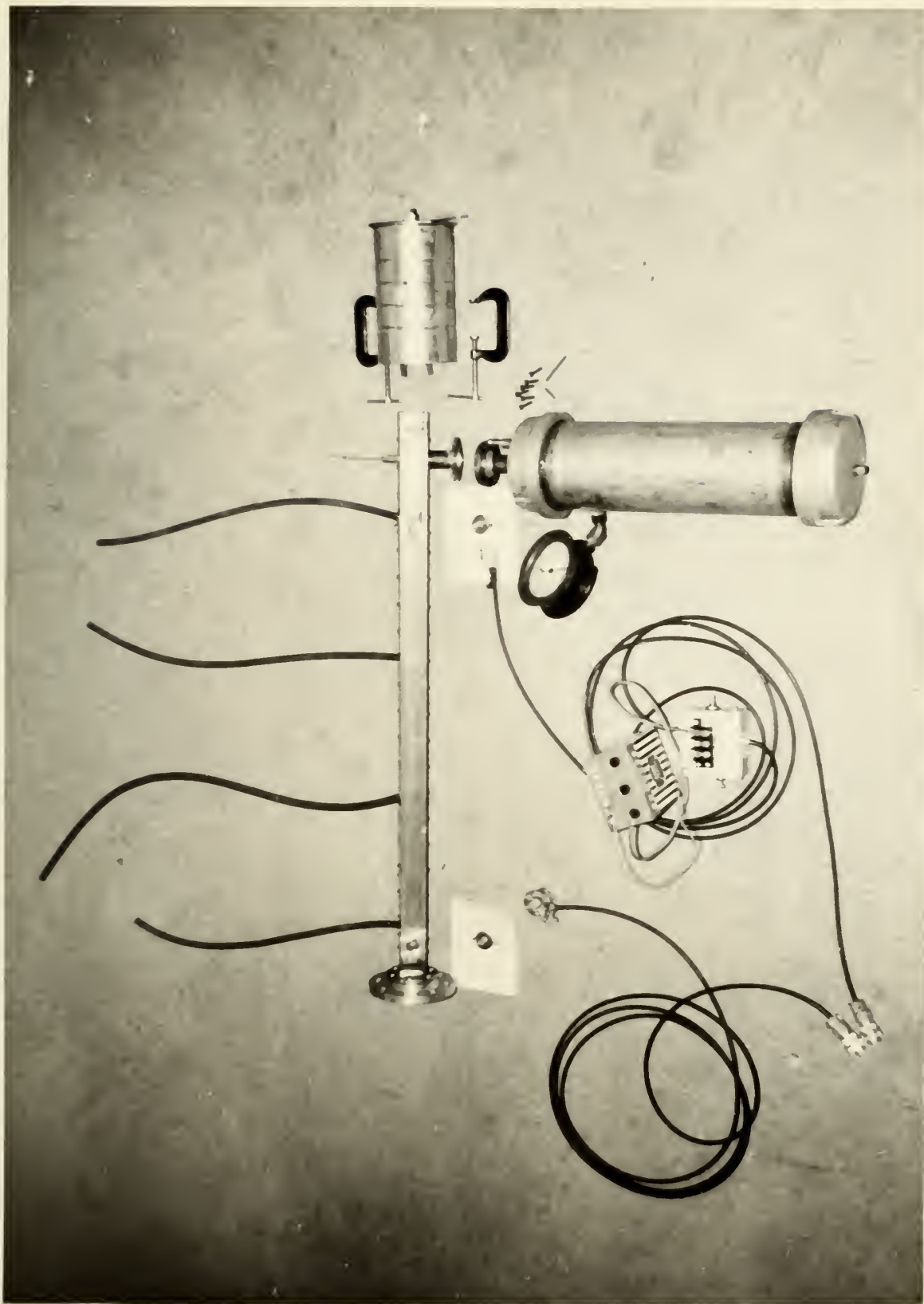


FIG.8

DISASSEMBLED VIEW OF TEST APPARATUS .

The electrical circuit to the left is that of the dynamic pick-up element with dummy gage mounted on the cable end near tube. Electrical system to right is for the pressure change sensing element. The cable connections at lower left plug directly into the Hathaway MRC 16 control unit.

Plastic diaphragms are inserted between the flanges of the divided pipe between explosion chamber and flow tube.



Max
No

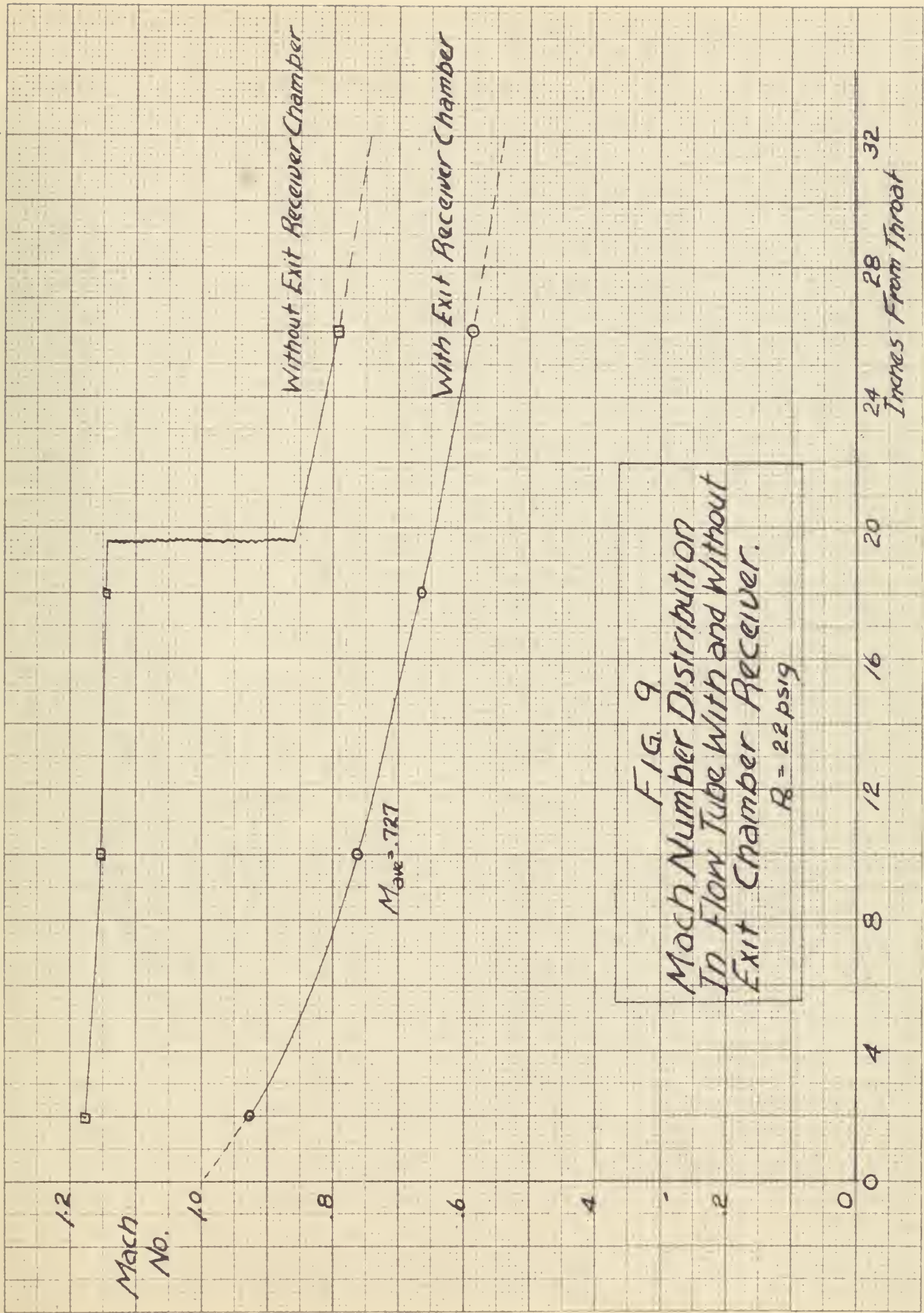


Fig. 10.
Pressure Tank Dial
Gage Calibration
U.S. Gage Co., Q-100 PSI
Using Dead Weight
Tester.

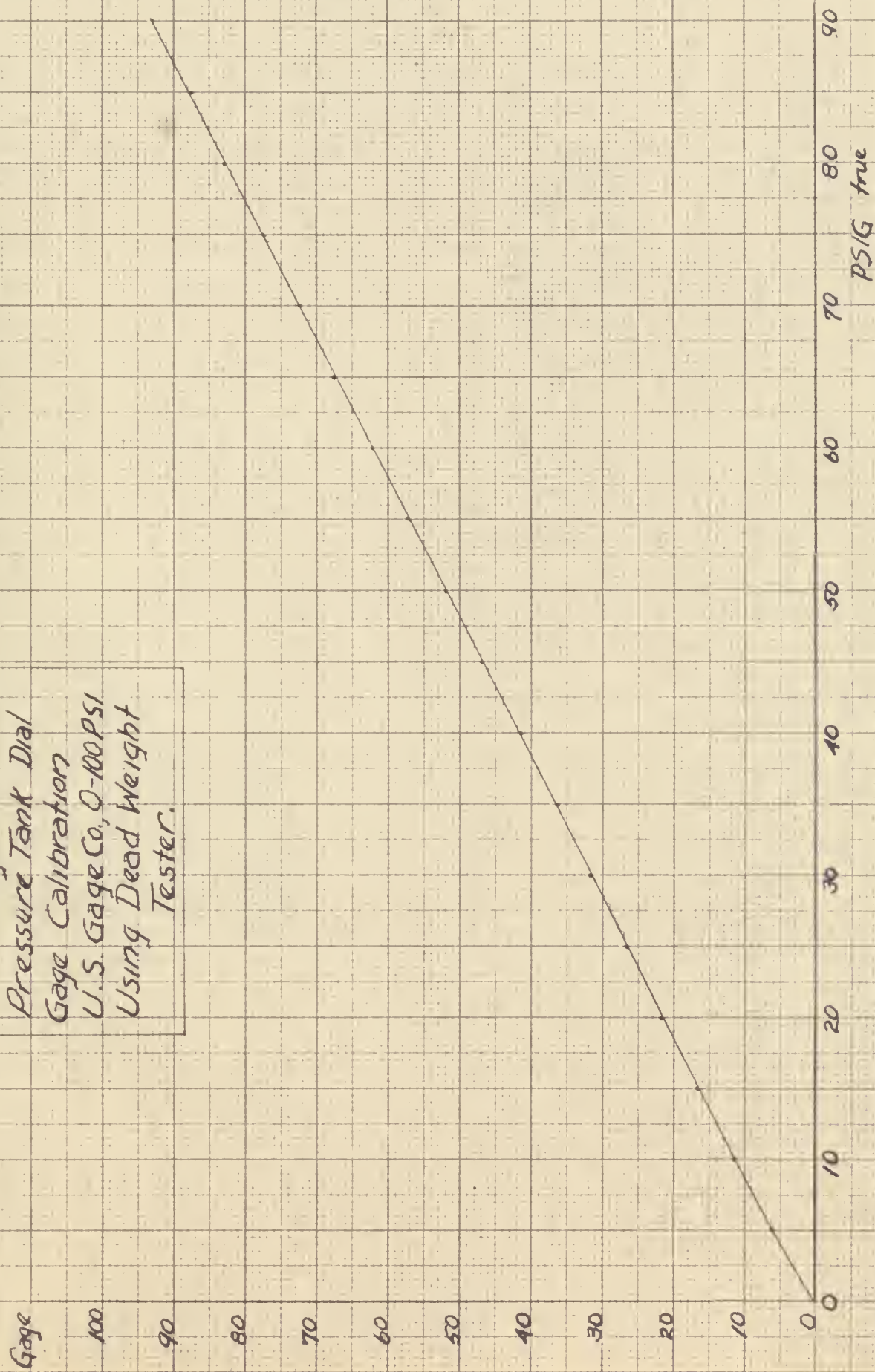


Fig. 11.
Flush-Mounted Dynamic
Pressure Pick-up
Calibration.

Gage Voltage 5v.
Attenuator $\frac{1}{2}$

Calibration:
2.61 psig/mm.
66.3 psig/in.

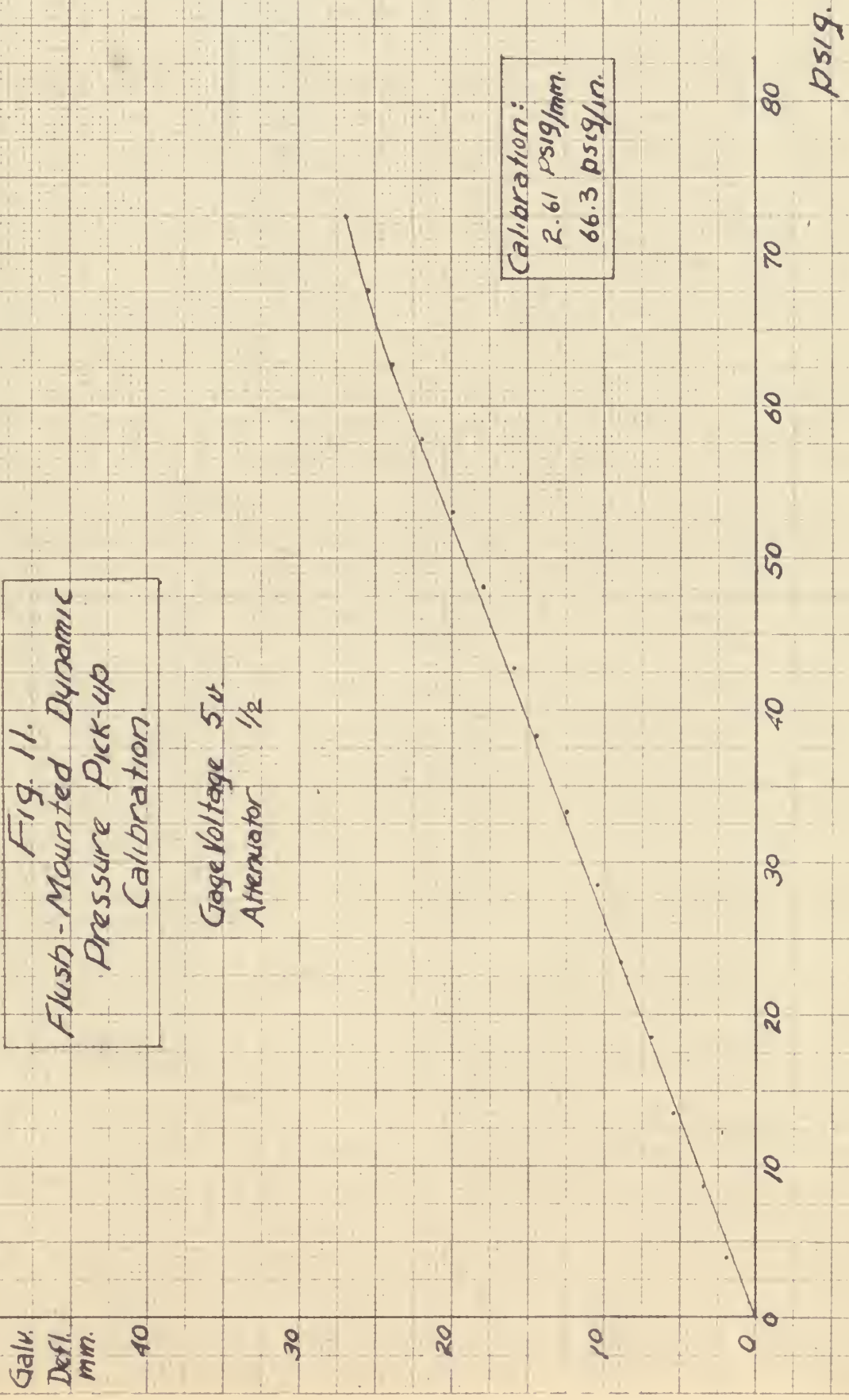
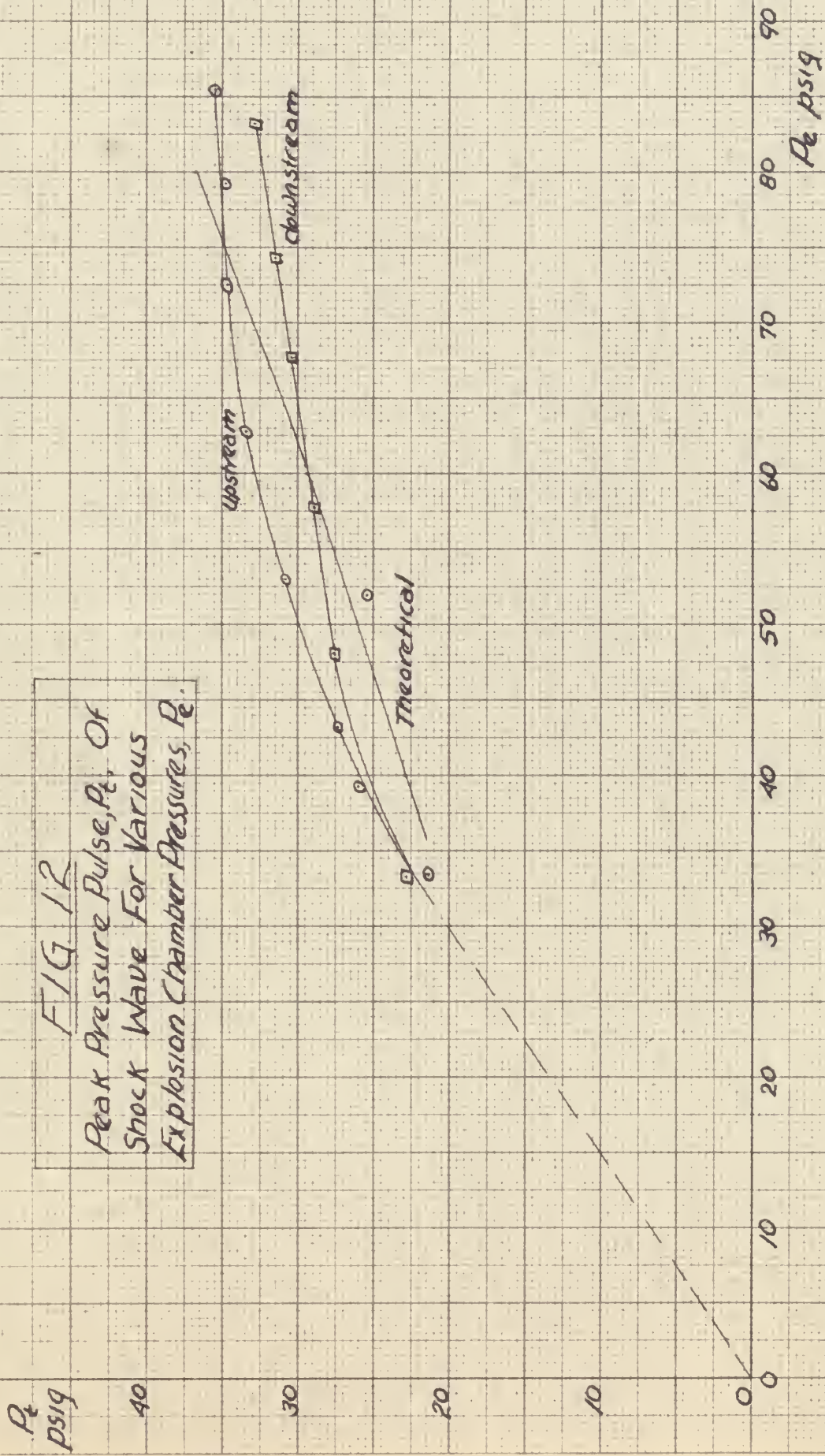
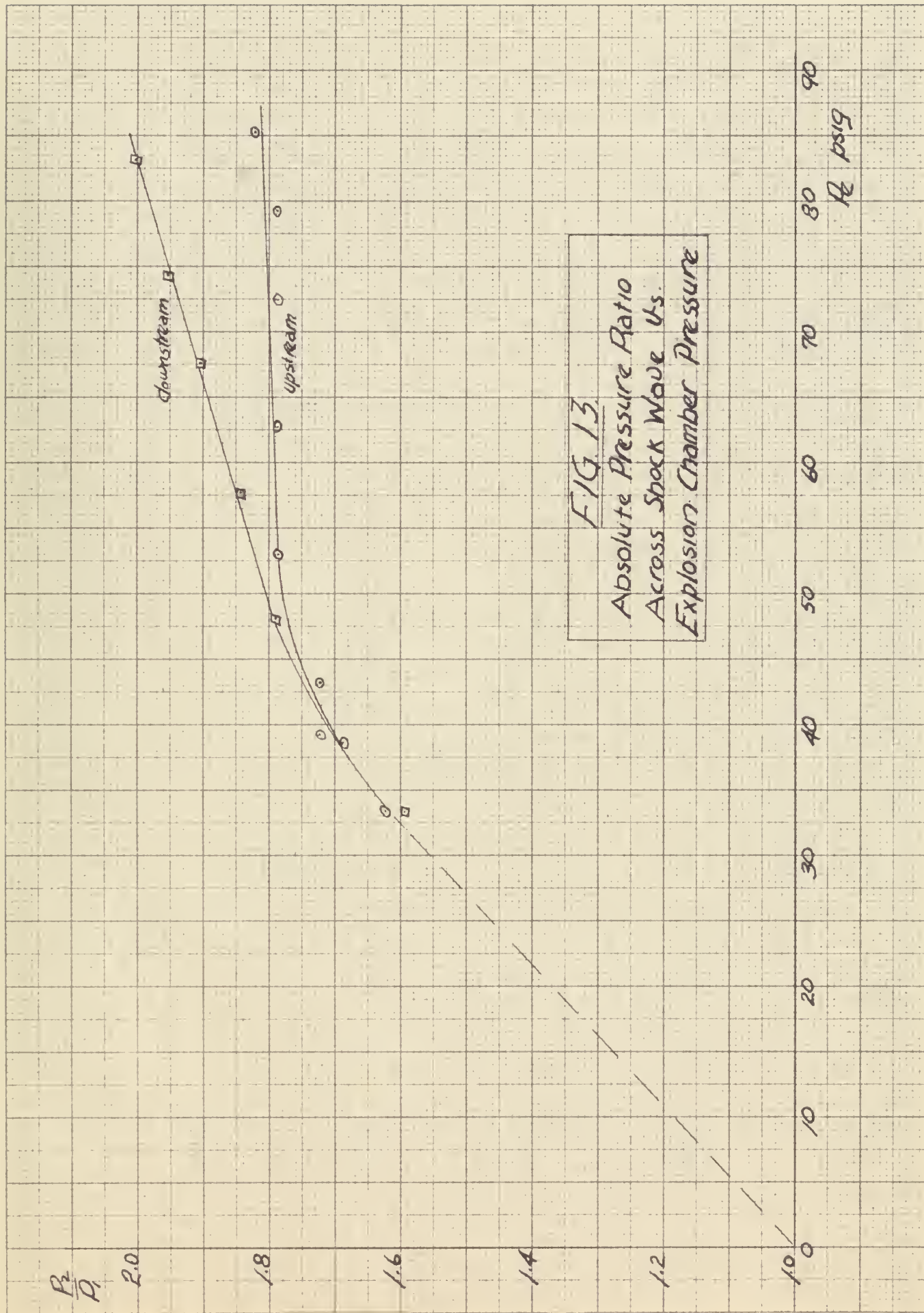


FIG 12
Peak Pressure Pulse, P_t , Of
Shock Wave For Various
Explosion Chamber Pressures, P_c .





Δt
Seconds

00450

00400

00350

00300

00250

00200

20

30

40

50

60

70

80

90

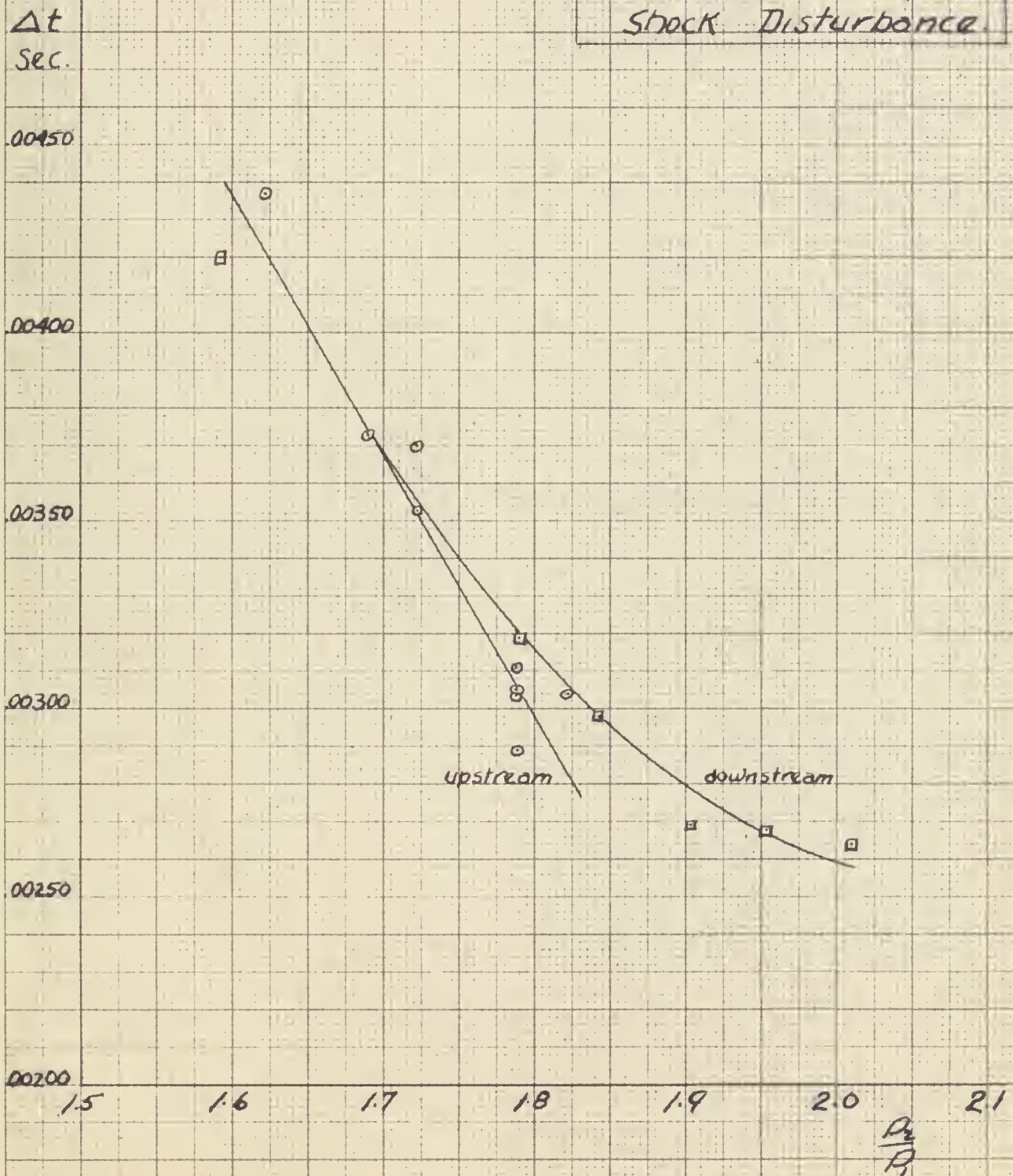
P psig

FIG 14

Time Required For Shock
Front To Traverse Test
Section vs. Explosion
Chamber Pressure.



FIG. 15.
Time Of Wave Traverse
vs. Pressure Ratio Across
Shock Disturbance.



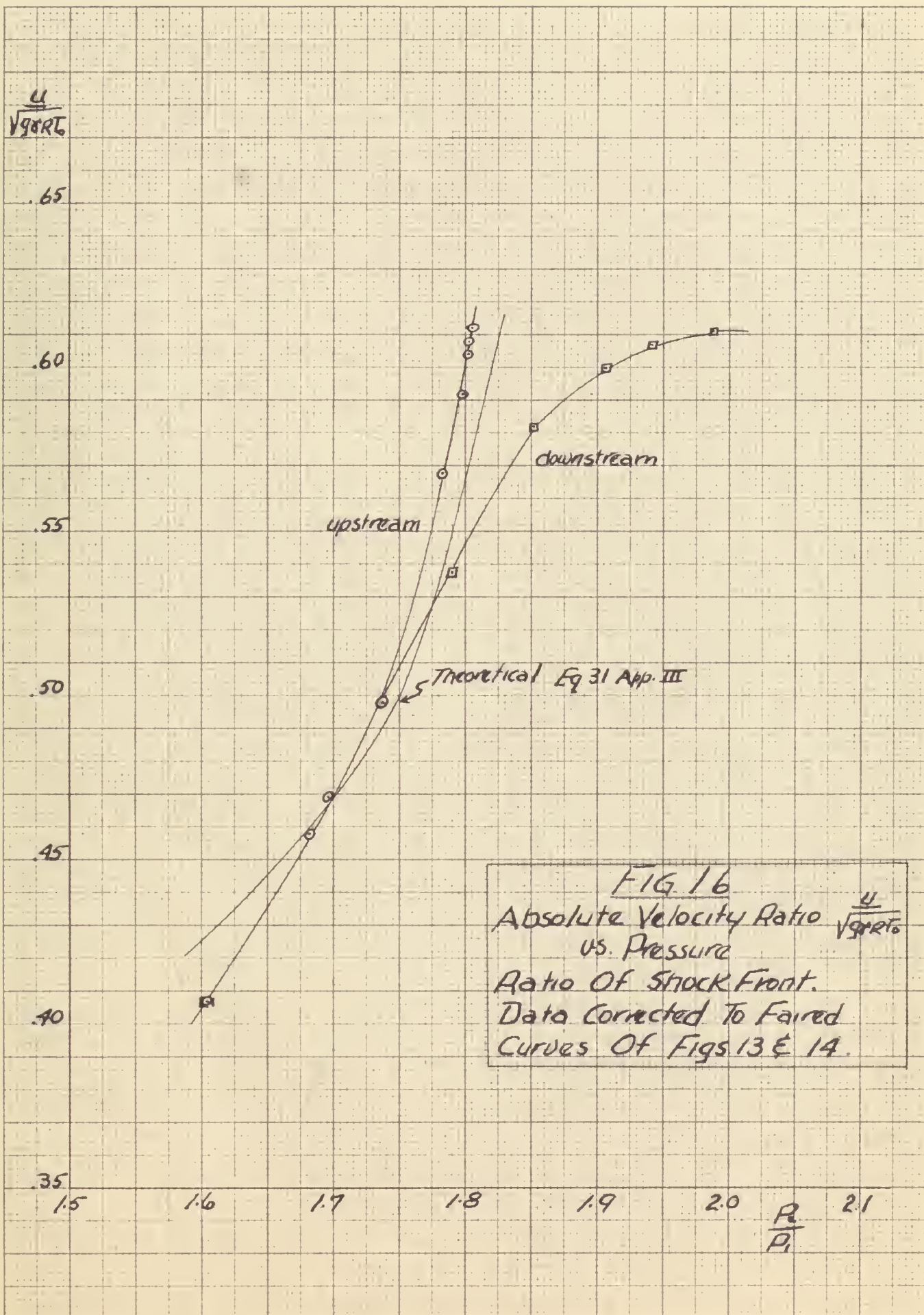


FIG. 16
 Absolute Velocity Ratio $\frac{u}{\sqrt{\gamma R T_0}}$
 vs. Pressure
 Ratio Of Shock Front.
 Data Corrected To Faired
 Curves Of Figs 13 & 14.

JUL 2
APR 23
APR 23
MAY 7

BINDERY
318
RENEWED
REMOVED

Thesis

J4

Jeffrey

18486

The propagation of medium
pressure disturbances in
high subsonic air flow.

★
JUL 2
APR 23
MAY 7

BINDERY
318
RENEWED
REMOVED

Thesis

J4

Jeffrey

18486

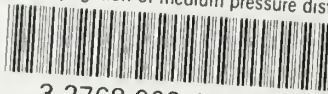
The propagation of medium pres-
sure disturbances in high sub-
sonic air flow.

Library
U. S. Naval Postgraduate School
Monterey, California



thesJ4

The propagation of medium pressure distu



3 2768 002 10054 7

DUDLEY KNOX LIBRARY